Impact of dust addition on the metabolism of Mediterranean plankton communities and carbon export under present and future conditions of pH and temperature

Frédéric Gazeau[1], France Van Wambeke[2], Emilio Marañón[3], María Pérez-Lorenzo[3], Samir Alliouane[1], Christian Stolpe[1], Thierry Blasco[1], Nathalie Leblond[4], Birthe Zäncker[5,6], Anja Engel[6], Barbara Marie[7], Julie Dinasquet[7,8], Cécile Guieu[1]

[1] Sorbonne Université, CNRS, Laboratoire d'Océanographie de Villefranche, LOV, 06230 Villefranche-sur-Mer, France

[2] Aix-Marseille Université, Université de Toulon, CNRS/INSU, IRD, Mediterranean Institute of Oceanography (MIO), UM 110, 13288, Marseille, France

[3] Department of Ecology and Animal Biology, Universidade de Vigo, 36310 Vigo, Spain

[4] Sorbonne Université, CNRS, Institut de la Mer de Villefranche, IMEV, 06230 Villefranche-sur-Mer, France

[5] The Marine Biological Association of the UK, PL1 2PB Plymouth, United Kingdom

[6] GEOMAR Helmholtz Centre for Ocean Research, Kiel, Germany

[7] CNRS, Sorbonne Université, Laboratoire d'Océanographie Microbienne, LOMIC, F-66650 Banyuls-sur-Mer, France

[8] Scripps Institution of Oceanography, University of California San Diego, USA

Correspondence to: Frédéric Gazeau (frederic.gazeau@imev-mer.fr)

Keywords: Mediterranean Sea; Atmospheric deposition; Plankton community metabolism; Carbon export; Ocean acidification; Ocean warming

Abstract

Although atmospheric dust fluxes from arid as well as human-impacted areas represent a significant source of nutrients to surface waters of the Mediterranean Sea, studies focusing on the evolution of the metabolic balance of the plankton community following a dust deposition event are scarce and none were conducted in the context of projected future levels of temperature and pH. Moreover, most of the experiments took place in coastal areas. In the framework of the PEACETIME project, three dust-addition perturbation experiments were conducted in 300-L tanks filled with surface seawater collected in the Tyrrhenian Sea (TYR), Ionian Sea (ION) and in the Algerian basin (FAST) onboard the R/V "*Pourquoi Pas?*" in late spring 2017. For each experiment, six tanks were used to follow the evolution of chemical and biological stocks, biological activity and particle export. The impacts of a dust deposition event simulated at their surface were followed under present environmental conditions and under a realistic climate change scenario for 2100 (ca. + 3 °C and -0.3 pH units). The tested waters were all typical of stratified oligotrophic conditions encountered in the open Mediterranean Sea at this period of the year, with low rates of primary production and a metabolic balance towards net heterotrophy. The release of nutrients after dust seeding had very contrasting impacts on the metabolism of the communities, depending on the station investigated. At TYR, the release of new nutrients was followed by a negative impact on both particulate and dissolved ^{14}C-based production rates, while heterotrophic bacterial production strongly increased, driving the community to an even more heterotrophic state. At ION and FAST, the efficiency of organic matter export due to mineral/organic aggregation processes was lower than at TYR and likely related to a lower quantity/age of dissolved organic matter present at the time of the seeding and a smaller

46 production of DOM following dust addition. This was also reflected by lower initial

47 concentrations in transparent exopolymer particles (TEP) and a lower increase in TEP

48 concentrations following the dust addition, as compared to TYR. At ION and FAST, both the

49 autotrophic and heterotrophic community benefited from dust addition, with a stronger relative

50 increase in autotrophic processes observed at FAST. Our study showed that the potential positive

51 impact of dust deposition on primary production depends on the initial composition and

52 metabolic state of the investigated community. This impact is constrained by the quantity of

53 nutrients added in order to sustain both the fast response of heterotrophic prokaryotes and the

54 delayed one of primary producers. Finally, under future environmental conditions, heterotrophic

55 metabolism was overall more impacted than primary production, with the consequence that all

56 integrated net community production rates decreased with no detectable impact on carbon

57 export, therefore reducing the capacity of surface waters to sequester anthropogenic CO_2.

Formatted: English (US)

Formatted: English (US)

Formatted: English (US)

Formatted: English (US)

Formatted: English (US)

Deleted: At ION and FAST, the efficiency of organic matter export due to mineral/organic aggregation processes was lower than at TYR likely related to a lower quantity/age of dissolved organic matter present at the time of the seeding.

Deleted: these stations

Formatted: English (US)

Deleted: potential

64

1. Introduction

Low Nutrient Low Chlorophyll (LNLC) areas represent 60% of the global ocean surface area (Longhurst et al., 1995; McClain et al., 2004). Although phytoplankton production in these areas is limited by the availability of nitrogen, phosphorus and iron, it accounts for 50% of global carbon export (Emerson et al., 1997; Roshan and DeVries, 2017). Atmospheric dust fluxes represent a significant source of these nutrients to surface waters in LNLC regions and as such could play a significant role in stimulating primary production (e.g. Bishop et al., 2002; Guieu et al., 2014b; Jickells and Moore, 2015), potentially increasing the efficiency of the biological pump in the sequestration of atmospheric CO_2. However, as heterotrophic prokaryotes have been shown to outcompete phytoplankton during nutrient addition experiments (e.g. Guieu et al., 2014a; Mills et al., 2008; Thingstad et al., 2005), dust deposition could induce even stronger enhancements of heterotrophic bacterial production and/or respiration rates thereby reducing net atmospheric CO_2 drawdown and the potential for carbon export outside the euphotic zone (Guieu et al., 2014b). Indeed, several experiments conducted in the Atlantic Ocean and in the Mediterranean Sea have shown a fast and dominant effect of dust additions on heterotrophic bacterioplankton metabolism (Herut et al., 2005, 2016; Lekunberri et al., 2010; Marañón et al., 2010; Pulido-Villena et al., 2008, 2014). However, to the best of our knowledge, no study focused on the evolution of the metabolic balance of the plankton community after such a dust event in the open sea. The metabolic balance (or net community production, NCP) is defined as the difference between gross primary production (GPP) of autotrophic organisms and community

96 respiration (CR) of both autotrophic and heterotrophic organisms, revealing the capacity of

97 surface waters to absorb atmospheric CO_2.

98   The Mediterranean Sea is a perfect example of LNLC regions and receives anthropogenic

99 aerosols originating from industrial and domestic activities from all around the basin and other

100 parts of Europe and pulses of natural inputs from the Sahara (Desboeufs, 2022). These

101 atmospheric depositions, mostly in the form of pulsed inputs (Loÿe-Pilot and Martin, 1996),

102 provide new nutrients (Guieu et al., 2010; Kouvarakis et al., 2001; Markaki et al., 2003; Ridame

103 and Guieu, 2002) to the surface waters with fluxes that are of the same order of magnitude as

104 riverine inputs (Powley et al., 2017). These significant nutrient enrichments likely support

105 primary production especially during the stratification period (Bonnet et al., 2005; Ridame and

106 Guieu, 2002). However, no clear correlation between dust and ocean color have been evidenced

107 from long series of satellite observations (Guieu and Ridame, 2020). This raises the question on

108 which compartment (autotrophic or heterotrophic) benefits the most from these transient relieves

109 in nutrient (N, P) limitation.

110   In response to ocean warming and increased stratification, LNLC areas are expected to

111 expand in the future (Irwin and Oliver, 2009; Polovina et al., 2008) due to lower nutrient supply

112 from sub-surface waters (Behrenfeld et al., 2006). Furthermore, dust deposition could increase in

113 the future due to desertification (Moulin and Chiapello, 2006), although so far the trend for

114 deposition remains uncertain because the drying of the Mediterranean basin might also induce

115 less wet deposition over the basin (Laurent et al., 2021). Nevertheless, whether the fluxes

116 increase or not in the coming decades and centuries, new nutrients from atmospheric sources will

117 play an important role in a surface mixed layer even more stratified and isolated from the deeper

118 nutrient-rich layer. The question remains on how plankton metabolism and carbon export would

Deleted: a system

Formatted: English (US), Subscript

Deleted: to sequester carbon via the biological pump

Deleted:

Deleted: (e.g. Bergametti et al., 1989; Desboeufs et al., 2018)

Formatted: English (US)

Formatted: English (US)

Formatted: English (US)

Formatted: English (US)

Formatted: English (US)

Formatted: English (US)

Deleted: ,

Deleted: however

Formatted: English (US)

Formatted: English (US)

Formatted: English (US)

Formatted: English (US)

Formatted: English (US)

Formatted: English (US)

Formatted: English (US)

Formatted: English (US)

Formatted: English (US)

Formatted: English (US)

125 respond in a warmer and more acidified ocean. Indeed, with an average annual anthropogenic

126 CO_2 uptake, during the period 2010 to 2019, of 2.5 ± 0.6 GtC (~22.9% of anthropogenic

127 emissions; Friedlingstein et al., 2020), the oceans substantially contribute towards slowing down

128 the increase in atmospheric CO_2 concentrations, and therefore towards limiting terrestrial and

129 ocean warming. However, this massive CO_2 input induces global changes in seawater chemistry

130 referred to as "ocean acidification" because increased CO_2 concentration lowers seawater pH

131 (i.e. increases its acidity).

132 Although the response of plankton metabolism to ocean warming has been shown to be

133 highly dependent on resource availability (Lewandowska et al., 2014), both for heterotrophic

134 bacteria (Lopez-Urrutia and Moran, 2007) and phytoplankton (Marañón et al., 2018), it has been

135 suggested that ocean warming will substantially weaken the ocean biological CO_2 sink in the

136 future as a consequence of stronger increase in remineralization than in photosynthesis

137 processes, following the metabolic theory of ecology (MTE; Brown et al., 2004; Gillooly et al.,

138 2001). Ocean acidification alone has been shown to exert no or very limited influence on

139 plankton metabolism in the Mediterranean Sea (Maugendre et al., 2017a; Mercado et al., 2014).

140 To the best of our knowledge, only Maugendre et al. (2015) studied the combined impact of

141 ocean warming and acidification on plankton metabolism in the Mediterranean Sea. They found

142 a very limited impact of ocean acidification on the plankton community and a positive impact of

143 warming on small phytoplankton species (e.g. Cyanobacteria) with a potential decrease of the

144 export and energy transfer to higher trophic levels. Their study was conducted under nutrient

145 depleted conditions (Maugendre et al., 2017b). Hence, there is still a need to assess the combined

146 impact of warming and acidification on the metabolic balance of plankton communities in this

147 region, following a transient relief in nutrient availability.

4

So far there has been no attempt to evaluate the evolution of plankton metabolism and carbon export following atmospheric deposition in the context of future levels of temperature and pH. Such experiments were conducted in the frame of the PEACETIME project (ProcEss studies at the Air-sEa Interface after dust deposition in the MEditerranean sea; http://peacetime-project.org/) during the cruise on board the R/V "*Pourquoi Pas?*" in May/June 2017 (Guieu et al., 2020a, b). The project aimed at extensively studying and parameterizing the chain of processes occurring in the Mediterranean Sea after atmospheric deposition, especially of Saharan dust, and to put them in perspective of on-going environmental changes. During this cruise, three perturbation experiments were conducted in 300-L tanks filled with surface seawater collected in the Tyrrhenian Sea (TYR), Ionian Sea (ION) and in the Algerian basin (FAST; Fig. 1). Six tanks were used to follow the evolution of chemical and biological stocks, biological activity and export, following a wet dust deposition event simulated at their surface, both under present environmental conditions and following a realistic climate change scenario for 2100 (ca. + 3 °C and -0.3 pH units; IPCC, 2013). A companion paper presents the general setup of the experiments and the impacts of dust under present and future environmental conditions on nutrients and biological stocks (Gazeau et al., 2021). In this paper, we show that the effects of dust deposition on biological stocks were highly different between the three investigated stations and could not be attributed to differences in their degree of oligotrophy but rather to the initial metabolic state of the community. We further demonstrated that ocean acidification and warming did not drastically modify the composition of the autotrophic assemblage with all groups positively impacted by warming and acidification. Here, we focus on the impacts of dust seeding on plankton metabolism (e.g. primary production, heterotrophic prokaryote production) and carbon export.

174

2. Material and Methods

2.1. General set-up

The general set-up of the experiments is fully detailed in Gazeau et al. (2021). Briefly,
three experiments were performed at the long duration stations TYR, ION and FAST during the
Peacetime cruise onboard R/V "*Le Pourquoi Pas?*" (Fig. 1). During these experiments (3 to 4
days each), seawater was incubated in 300-L tanks (Fig. S1) installed in a temperature-controlled
container, in which the irradiance spectrum and intensity can be finely controlled and in which
future ocean acidification and warming conditions can be fully reproduced. The tanks were made
of high-density polyethylene (HDPE) and were trace-metal free in order to avoid contaminations,
with a height of 1.09 m, a diameter of 0.68 m, a surface area of 0.36 m^2 and a volume of 0.28 m^3.
The conical base of the tanks was equipped with a sediment trap that was left open during the
duration of the experiments and removed at the end. The experimental protocol comprised two
unmodified control tanks (C1 and C2), two tanks enriched with Saharan dust (D1 and D2) and
two tanks enriched with Saharan dust and maintained simultaneously under warmer (+ 3 ºC) and
acidified (-0.3 pH unit) conditions (G1 and G2). At the three stations, tanks were always filled at
the end of the day before the start of the experiments: TYR (17/05/2017), ION (25/05/2017) and
FAST (02/06/2017). The tanks were filled by means of a large peristaltic pump (Verder© VF40
with EPDM hose, flow of 1200 L h^{-1}) collecting seawater below the base of the boat (depth of ~
5 m), used to supply continuously surface seawater to a series of instruments during the entire
campaign. While filling the tanks, seawater was sampled for the measurements of selected
parameters (sampling time = t-12h). After filling the tanks, seawater was slowly warmed

6

197 overnight using 500 W heaters, controlled by temperature-regulation units (COREMA©), in G1

198 and G2 to reach an offset of + 3 °C. ^{13}C-bicarbonate was added to all tanks at 4:00 am (all times

199 in local time) and G1 and G2 were acidified by addition of CO_2-saturated filtered (0.2 μm)

200 seawater (~1.5 L in 300 L; collected when filling the tanks at each station) at 4:30 am to reach a

201 pH offset of -0.3. Sampling for many parameters took place prior to dust seeding (sampling time

202 = t0). Dust seeding was performed between 7:00 and 9:00 in tanks D1, D2, G1 and G2. The same

203 dust analog was used and the same dust flux was simulated as for the DUNE 2009 experiments

204 described in Desboeufs et al. (2014). Briefly, the fine fraction (< 20 μm) of Saharan soils

205 collected in southern Tunisia, which is a major source of dust deposition over the northwestern

206 Mediterranean basin, was used in the seeding experiments. The particle size distribution showed

207 that 99% of particles had a size smaller than 0.1 μm, and that particles were mostly made of

208 quartz (40%), calcite (30%) and clay (25%; Desboeufs et al., 2014). This collected dust

209 underwent an artificial chemical aging process by addition of nitric and sulfuric acid (HNO_3 and

210 H_2SO_4, respectively) to mimic cloud processes during atmospheric transport of aerosol with

211 anthropogenic acid gases (Guieu et al., 2010, and references therein). To mimic a wet flux event

212 of 10 g m^{-2}, 3.6 g of this analog dust were quickly diluted into 2 L of ultrahigh-purity water

213 (UHP water; 18.2 MΩ cm^{-1} resistivity), and sprayed at the surface of the tanks using an all-

214 plastic garden sprayer (duration = 30 min). The intensity of this simulated wet deposition event

215 (i.e. 10 g m^{-2}) represents a high but realistic scenario, as several studies reported even higher

216 short wet deposition events in this area of the Mediterranean Sea (Bonnet and Guieu, 2006;

217 Loÿe-Pilot and Martin, 1996; Ternon et al., 2010).

218   Depending on the considered parameter or process, seawater sampling was conducted 1 h

219 (t1h), 6 h (t6h), 12 h (t12h), 24 h (t24h), 48 h (t48h) and 72 h (t72h) after dust additions in all

225 three experiments with an additional sample after 96 h (t96h) at FAST). Acid-washed silicone

226 tubes were used for transferring the water collected from the tanks to the different vials or

227 containers.

2.2. Stocks

2.2.1. Dissolved and particulate organic carbon

230   The concentration of dissolved organic carbon (DOC) was determined from duplicate 10

231 mL GF/F (pre-combusted, Whatman©) filtered subsamples that were transferred to pre-

232 combusted glass ampoules, acidified with H_3PO_4 (final pH = 2) and sealed. The sealed glass

233 ampoules were stored in the dark at room temperature until analysis at the Laboratoire

234 d'Océanographie Microbienne (LOMIC). DOC measurements were performed on a Shimadzu©

235 TOC-V-CSH (Benner and Strom, 1993). Prior to injection, DOC samples were sparged with

236 CO_2-free air for 6 min to remove inorganic carbon. Sample (100 μL) were injected in triplicate

237 and the analytical precision was 2%. Standards were prepared with acetanilid.

238   Seawater samples for measurements of particulate organic carbon concentrations (POC; 2

239 L) were taken at t-12h, t0, t12h, t24h, t48h and t72h (or t96h for station FAST), filtered on pre-

240 combusted GF/F membranes, dried at 60 °C and analyzed at the Laboratoire d'Océanographie de

241 Villefranche (LOV, France) following decarbonatation with a drop of HCl 2N, on an elemental

242 analyzer coupled with an isotope ratio mass spectrometer (EA-IRMS; Vario Pyrocube-Isoprime

243 100, Elementar©). A caffeine standard (IAEA-600) was used to calibrate the EA-IRMS.

2.2.2. Total hydrolysable carbohydrates and amino acids

249   For total hydrolysable carbohydrates and amino acids, samples were taken at t0, t6h,

250 t24h, t48h and t72h at all stations. For total hydrolysable carbohydrates (TCHO) > 1 kDa,

251 samples (20 mL) were filled into pre-combusted glass vials (8 h, 500 °C) and stored at -20 °C

252 pending analysis. Prior to analysis, samples were desalted with membrane dialysis (1 kDa

253 MWCO, Spectra Por) at 1 °C for 5 h. Samples were subsequently hydrolyzed for 20 h at 100 °C

254 with 0.8 M HCl final concentration followed by neutralization using acid evaporation (N_2, for 5

255 h at 50 °C). TCHO were analysed at GEOMAR using high performance anion exchange

256 chromatography with pulsed amperometric detection (HPAEC-PAD), on a Dionex© ICS 3000

257 ion chromatography system following the procedure of Engel and Händel (2011). Two replicates

258 per TCHO sample were analyzed. The variation coefficient between duplicate measurements was

259 7% on average.

260   For total hydrolysable amino acids (TAA), samples (5 mL) were filled into pre-

261 combusted glass vials (8 h, 500 °C) and stored at -20 °C. Samples were hydrolyzed at 100 °C for

262 20 h with 1 mL 30% HCl (Suprapur®, Merck) added to 1 mL of sample, and neutralized by acid

263 evaporation under vacuum at 60 °C in a microwave. Samples were analyzed by high

264 performance liquid chromatography (HPLC) using an Agilent 1260 HPLC system following a

265 modified version of established methods (Dittmar et al., 2009; Lindroth and Mopper, 1979).

266 Separation of 13 amino acids with a C18 column (Phenomenex Kinetex, 2.6 µm, 150 x 4.6 mm)

267 was obtained after in-line derivatization with o-phthaldialdehyde and mercaptoethanol. A

268 gradient with solvent A containing 5 % acetonitrile (LiChrosolv, Merck, HPLC gradient grade)

269 in sodium dihydrogenphosphate (Suprapur®, Merck) buffer (pH 7.0) and solvent B being

270 acetonitrile was used for analysis. A gradient from 100% solvent A to 78% solvent A was

271 produced in 50 min. Two replicates per TAA sample were analyzed. The variation coefficient

Formatted: English (US)

Formatted: English (US)
Formatted: English (US)

Deleted: ¶

Formatted: English (US)
Formatted: English (US)

273 between duplicate measurements was 8% on average. For TCHO and TAA, instrument blanks

274 were performed with MilliQ water. The detection limit was calculated as 3x the blank value,

275 which is ~1 nmol L^{-1} for both parameters.

2.2.3. Transparent exopolymer particles

277   Samples for transparent exopolymer particles (TEP) were taken at t0, t24h and t72h at all

278 stations. The abundance and area of TEP were microscopically measured following the

279 procedure given in Engel (2009). Samples of 10-50 mL were directly filtered under low vacuum

280 (< 200 mbar) onto a 0.4 µm Nucleopore membrane (Whatman©) filter, stained with 1 mL Alcian

281 Blue solution (0.2 g l^{-1} w/v) for 3 s and rinsed with MilliQ water. Filters were mounted on

282 Cytoclear© slides and stored at -20 °C until analysis. Two filters per sample with 30 images each

283 were analyzed using a Zeiss Axio Scope.A1 (Zeiss©) and an AxioCam MRc (Zeiss©). The

284 pictures with a resolution of 1388 x 1040 pixels were saved using AxioVision LE64 Rel. 4.8

285 (Zeiss©). All particles larger than 0.2 μm^2 were analyzed. ImageJ© and R were subsequently

286 used for image analysis (Schneider et al., 2012). The coefficients of variation between duplicate

287 filters averaged 28%.

288   Filters prepared with 10 mL MilliQ water instead of samples served as a blank. Blanks

289 were always <1% of sample values. The carbon content of TEP (TEP-C) was estimated after

290 Mari (1999) using the size-dependent relationship:

291 $TEP\text{-}C = a \sum_i n_i r_i^D$ (1)

292 with n_i being the number of TEP in the size class i and r_i being the mean equivalent spherical

293 radius of the size class. The constant $a = 0.25 * 10^{-6}$ (µg C) and the fractal dimension of

296 aggregates $D = 2.55$ were used as proposed by Mari (1999). To relate to organic carbon

297 concentration in seawater, data for TEP-C are given as µmol L^{-1}.

2.3. Processes

2.3.1. Dissolved and particulate ^{14}C incorporation rates

300   The photosynthetic production of particulate (< 0.2-2 µm and > 2 µm size fractions) and

301 dissolved organic matter was determined from samples taken at t0, t24h, t48h and t72h (or t96h

302 at station FAST) with the ^{14}C-uptake technique. From each tank, four polystyrene bottles (70

303 mL; three light and one dark bottles) were filled with sampled seawater and amended with 40

304 µCi of NaH^{14}CO$_3$. Bottles were incubated for 8 h in two extra 300 L tanks maintained under

305 similar light and temperature regimes as in the experimental tanks (ambient temperature for C1,

306 C2, D1 and D2 and ambient temperature + 3 °C for G1 and G2). Incubations were terminated by

307 sequential filtration of the sample through polycarbonate filters (pore sizes 2 µm and 0.2 µm, 47

308 mm diameter) using low-pressure vacuum. Filters were exposed for 12 h to concentrated HCl

309 fumes to remove non-fixed, inorganic ^{14}C, and then transferred to 4 mL plastic scintillation vials

310 to which 3.5 mL of scintillation cocktail (Ultima Gold XR, Perkin Elmer©) were added. For the

311 measurement of dissolved primary production, a 5 mL aliquot of each sampling bottle was

312 filtered, at the end of incubation, through a 0.2 µm polycarbonate filter (25 mm diameter). This

313 filtration was conducted, under low-pressure vacuum, in a circular filtration manifold that allows

314 the recovery of the filtrate into 20 mL scintillation vials. The filtrates were acidified with 200 µL

315 of 50% HCl and maintained in an orbital shaker for 12 h. Finally, 15 mL of liquid scintillation

316 cocktail was added to each sample. All filter and filtrate samples were measured onboard in a

11

318   liquid scintillation counter (Packard© 1600 TR). ^{14}C-based production rates (PP; in µg C L^{-1} h^{-1})

319   were calculated as:

320     $$PP = C_T \times \left(\frac{DPM_{sample} - DPM_{dark}}{DPM_{added} \times t} \right) \qquad (2)$$

321   where C_T is the concentration of total dissolved inorganic carbon (µg C L^{-1}), DPM_{sample} and

322   DPM_{dark} are the radioactivity counts in the light and dark bottle, respectively, DPM_{added} is the

323   radioactivity added to each sample, and t is the incubation time (h).

324   The percentage extracellular release (PER%) was calculated as:

325     $$PER\% = \frac{PPd}{PPd + PPp} \times 100 \qquad (3)$$

326   where PPd refers to ^{14}C-based dissolved production and PPp refers to ^{14}C-based particulate

327   production (sum of < 2 and > 2 µm size fractions).

2.3.2. Integrated ^{13}C incorporation

329   Addition of ^{13}C-bicarbonate (NaH^{13}CO$_3$ 99%; Sigma-Aldrich©) was performed in each

330   tank before t0 in order to increase the isotopic level (δ^{13}C signature) of the dissolved inorganic

331   carbon pool to ca. 350‰. We followed the time evolution of the δ^{13}C signature in dissolved

332   inorganic carbon (δ^{13}C-C_T), dissolved organic carbon (δ^{13}C-DOC) and particulate organic carbon

333   pools (δ^{13}C-POC). For the analysis of the actual δ^{13}C-C_T, 60 mL of sampled seawater (at t-12h,

334   t0, t12h, t24h, t48h and t72h; + t96h at station FAST) was gently transferred to glass vials

335   avoiding bubbles. Vials were sealed after being poisoned with 12 µL saturated HgCl$_2$ and stored

336   upside-down at room temperature in the dark pending analysis. At the University of Leuven, a

337   helium headspace (5 mL) was created in the vials and samples were acidified with 2 mL of

12

340   phosphoric acid (H_3PO_4, 99%). Samples were left to equilibrate overnight to transfer all C_T to

341   gaseous CO_2. Samples were injected in the carrier gas stream of an EA-IRMS (Thermo©

342   EA1110 and Delta V Advantage), and data were calibrated with NBS-19 and LSVEC standards

343   (Gillikin and Bouillon, 2007).

344   At the same frequency as for $\delta^{13}C$-C_T, samples for $\delta^{13}C$-DOC were filtered online (see

345   above), transferred to 40 mL pre-cleaned borosilicate amber EPA vials with septa caps (PTFE-

346   lined silicone) and stored in the dark pending analysis at the Ján Veizer Stable Isotope

347   Laboratory (Ottawa, Canada).

348   At t-12h, t0, t12h, t24h, t48h and t72h (or t96h at station FAST), the $\delta^{13}C$-POC was

349   obtained based on the same measurements as described above for POC, on an elemental analyzer

350   coupled with an isotope ratio mass spectrometer (EA-IRMS; Vario Pyrocube-Isoprime 100,

351   Elementar©).

352   Carbon isotope data are expressed in the delta notation (δ) relative to Vienna Pee Dee

353   Belemnite (VPDB) standard (REF?). The carbon isotope ratio was calculated as:

354    $$R_{sample} = \left(\frac{\delta^{13}C_{sample}}{1000} + 1\right) \times R_{VPDB} \qquad (4)$$

355   with $R_{VPDB} = 0.011237$.

13

2.3.2. Community metabolism (oxygen light-dark method)

At the same frequency as for ^{14}C incorporation, from each tank, a volume of 2 L was sampled in plastic bottles and distributed in 15 biological oxygen demand (BOD; 60 mL) borosilicate bottles. Five BOD bottles were immediately fixed with Winkler reagents (initial O_2 concentrations), five BOD bottles were incubated in the dark for the measurement of community respiration (CR) in two incubators maintained respectively at ambient temperature for C1, C2, D1 and D2 and at ambient temperature + 3 °C for G1 and G2. Additionally, five BOD bottles were incubated for the measurement of net community production (NCP) in the same tanks as described above for ^{14}C-incorporation. Upon completion of the incubations (24 h), samples were fixed with Winkler reagents. Within one day, O_2 concentrations were measured using an automated Winkler titration technique with potentiometric endpoint detection. Analyses were performed on board with a Metrohm© Titrando 888 and a redox electrode (Metrohm© Au electrode). Reagents and standardizations were similar to those described by Knap et al. (1996). NCP and CR were estimated by regressing O_2 values against time, and CR was expressed as negative values. Gross primary production (GPP) was calculated as the difference between NCP and CR. The combined standard errors were calculated as:

$$SE_{xy} = \sqrt{SE_x^2 + SE_y^2} \qquad (5)$$

14

2.3.4. Heterotrophic prokaryotic production and ectoenzymatic activities

At all sampling times, heterotrophic bacterial production (BP, *sensus stricto* referring to heterotrophic prokaryotic production) was determined onboard using the microcentrifuge method with the [3]H- leucine (^{3}H-Leu) incorporation technique to measure protein production (Smith and Azam, 1992). The detailed protocol is in Van Wambeke et al. (2021). Briefly, triplicate 1.5 mL samples and one blank were incubated in the dark for 1-2 h in two thermostated incubators maintained respectively at ambient temperature for C1, C2, D1 and D2 and at ambient temperature +3 °C for G1 and G2. Incubations were ended by the addition of TCA to a final concentration of 5%, followed by three runs of centrifugation at 16000 g for 10 min. Pellets were rinsed with TCA 5% and ethanol 80%. A factor of 1.5 kg C mol leucine[-1] was used to convert the incorporation of leucine to carbon equivalents, assuming no isotopic dilution (Kirchman et al., 1993).

Ectoenzymatic activities were measured fluorometrically, using fluorogenic model substrates that were L-leucine-7-amido-4-methyl-coumarin (Leu-MCA) and 4 methylumbelliferyl – phosphate (MUF-P) to track aminopeptidase activity (LAP) and alkaline phosphatase activity (AP), respectively (Hoppe, 1983). Stocks solutions (5mM) were prepared in methycellosolve and stored at -20 °C. Release of the products of LAP and AP activities, MCA and MUF, were followed by measuring increase of fluorescence (exc/em 380/440 nm for MCA and 365/450 nm for MUF, wavelength width 5 nm) in a VARIOSCAN LUXmicroplate reader calibrated with standards of MCA and MUF solutions. For measurements, 2 mL of unfiltered samples from the tanks were supplemented with 100

398 µL of a fluorogenic substrate solution diluted so that different concentrations were

399 dispatched in a black 24-well polystyrene plate in duplicate (0.025, 0.05, 0.1, 0.25, 0.5, 1 µM

400 for MUF-P, 0.5, 1, 5, 10, 25 µM for MCA-leu). Incubations were carried out in the same

401 thermostatically controlled incubators than those used for BP and reproducing temperature

402 levels in the experimental tanks. Incubations lasted up to 12 h long with a reading of

403 fluorescence every 1 to 2 h, depending on the intended activities. The rate was calculated

404 from the linear part of the fluorescence versus time relationship. Boiled-water blanks were

405 run to check for abiotic activity. From varying velocities obtained, we determined the

406 parameters Vm (maximum hydrolysis velocity) and Km (Michaelis-Menten constant which

407 reflects enzyme affinity for the substrate) by fitting the data using a non-linear regression on

408 the following equation:

409 $$V = V_m \ x \ \frac{S}{K_m + S} \tag{6}$$

410 where V is the hydrolysis rate and S the fluorogenic substrate concentration added.

2.3.5. Inorganic and organic material export

412   At the end of each experiment (t72h for TYR and ION and t96 h for FAST, after artificial

413 dust seeding), the sediment traps were removed, closed and stored with formaldehyde 4%. Back

414 in the laboratory, after the swimmers were removed, the samples were rinsed to remove the salts

415 and then freeze-dried. The total amount of material collected was first weighted to measure the

416 total exported flux. Several aliquots were then weighted to measure the following components:

417 total carbon and organic carbon, lithogenic and biogenic silicates and calcium. Total carbon was

418 measured on an elemental analyzer coupled with an isotope ratio mass spectrometer (EA-IRMS;

16

419 Vario Pyrocube-Isoprime 100, Elementar©). Particulate organic carbon (POC) was measured in

420 the same way after removing inorganic carbon by acidification with HCl 2N. Particulate

421 inorganic carbon (PIC) was obtained by subtracting particulate organic carbon from particulate

422 total carbon. Calcium concentrations were measured by ICP-OES (Inductively Coupled Plasma -

423 Optic Emission Spectrometry; Perkin-Elmer© Optima 8000) on acid digested samples (the

424 organic matrix was removed by HNO_3 while the mineral aluminosilicate matrix was eliminated

425 with HF). Biogenic silica (BSi) and Lithogenic silica (LSi) were measured by colorimetry

426 (Analytikjena© Specor 250 plus spectrophotometer) after a NaOH/HF digestion, respectively

427 (Mosseri et al., 2005). The carbonate fraction of the exported material was determined from

428 particulate calcium concentrations ($\%CaCO_3$ = 5/2 x (%Ca). The organic matter fraction was

429 calculated as 2 x %POC (Klaas and Archer, 2002) The lithogenic fraction was calculated as

430 [total mass – (organic matter + $CaCO_3$ + opal) and was very comparable to the lithogenic

431 fraction calculated from LSi (taking Si concentration in dust analog used for seeding from

432 Desboeufs et al., 2014; ca. 11.9%). In the controls, the amount of material exported was low and

433 the entire content of the traps was filtered in order to measure total mass and organic matter mass

434 fluxes.

435
436 ## 2.4. Data processing

437 All metabolic rates were integrated over the duration of the experiments using trapezoidal

438 integrations and the relative changes (in %) in tanks D and G as compared to the controls

439 (average between C1 and C2) were computed following:

440 Relative change = $\left(\frac{Rate_{Treatment} - Rate_{Controls}}{Rate_{Controls}}\right)$ x 100 (7)

17

444   Where Rate$_{Treatment}$ is the integrated rate measured in treatments D and G (D1, D2, G1 or G2) and

445   Rate$_{Controls}$ is the averaged integrated rates between the duplicate controls (treatment C). Daily

446   rates of ^{14}C-based production were computed from hourly rates assuming a 14 h daylight period.

447   As incubations performed from samples taken at t0 (before dust addition) do not represent what

448   happened in the tanks between t0 and t24h, as a first assumption, we considered a linear

449   evolution between these rates and those measured from samples at t24h, and recomputed an

450   average value for the time interval t0 - t24 h. At FAST, no incubations were performed for ^{14}C

451   incorporation and oxygen metabolism between t72h and t96h, again an average rate between

452   rates measured from samples taken at t48h and t96h was used for this time interval. Since

453   bacterial respiration rates were not measured, bacterial growth efficiency (BGE, expressed as a

454   percentage) was estimated based on BP (carbon units) and community respiration (CR, oxygen

455   units). As BP was determined more often than CR during the first 48 h, hourly BP rates were

456   integrated using trapezoidal integrations during the time period when CR was measured. We

457   assumed that heterotrophic prokaryotes were responsible for 70% of CR (BR/CR ratio; Lemée et

458   al., 2002) and used a respiratory quotient (RQ) of 0.8 (del Giorgio and Williams, 2005),

459   following the equation:

460     $$BGE = \left(\frac{BP}{CR \times \frac{BR}{CR}\text{ratio} \times RQ + BP} \right) \times 100 \quad\quad\quad (8)$$

461   When BP varied following an exponential growth, we calculated growth rates (μ_{BP}) from linear

462   least square regression of ln BP rates versus time.

3. Results

3.1. Initial conditions

Initial conditions in terms of the chemical and biological standing stocks measured while filling the tanks at the three stations are fully described in Gazeau et al. (2021). Briefly, the three experiments were conducted with surface seawater collected during stratified oligotrophic conditions typical of the open Mediterranean Sea at this period of the year (Table 1). Nevertheless, a dust event took place nine days before sampling at station TYR as evidenced from particulate inventory of lithogenic proxies (Al, Fe) in the water column (Bressac et al., 2021), likely stimulating phytoplankton growth before the start of the experiment. Nitrate + nitrite (NO_x) concentrations were maximal at station FAST with a NO_x to dissolved inorganic phosphate (DIP) molar ratio of ~ 4.6. Very low NO_x concentrations were observed at stations TYR and ION (14 and 18 nmol L^{-1}, respectively). DIP concentrations were the highest at station TYR (17 nmol L^{-1}) and the lowest at the most eastern station (ION, 7 nmol L^{-1}). Consequently, the lowest NO_x:DIP ratio was measured at TYR (0.8), compared to ION and FAST (2.8 and 4.6, respectively). Silicate ($Si(OH_4)$) concentrations were similar at TYR and ION (~1 μmol L^{-1}) and the lowest at FAST (~0.6 μmol L^{-1}). Both POC and DOC concentrations were the highest at station TYR (12.9 and 72.2 μmol L^{-1}, respectively) and the lowest at FAST (6.0 and 69.6 μmol L^{-1}, respectively). Very low and similar concentrations of chlorophyll *a* were measured at the three stations (0.063 - 0.072 μg L^{-1}). Phytoplankton communities at stations TYR and ION were dominated by Prymnesiophytes followed by Cyanobacteria, while, at station FAST, the phytoplanktonic community was clearly dominated by photosynthetic prokaryotes. At all three stations, the proportion of pigments representative of larger species was very small (< 5%;

486   Gazeau et al., 2021). Heterotrophic prokaryotes were the most abundant at station FAST (6.15 x

487   10^5 cells mL^{-1}) and the least abundant at station ION (2.14 x 10^5 cells mL^{-1}).

488   Relatively similar ^{14}C-based particulate production rates were measured at the start of the

489   experiments (t0) in the control tanks (C1 and C2) at station ION and FAST (ca. 0.014 - 0.015 µg

490   C L^{-1} h^{-1}). At both stations, ca. 80% of the production was attributed to larger (> 2 µm) cells and

491   the percentage of extracellular release (%PER) did not exceed 45%. Lower rates were estimated

492   at station TYR (total particulate production of 0.08 µg C L^{-1} h^{-1}) from which 87.5% was due to

493   large cells > 2 µm. A larger amount of ^{14}C incorporation was released as dissolved organic

494   matter at station TYR compared to the two other stations (PER ca. 60%). Metabolic balance

495   derived from oxygen measurements showed that, at all three stations, the community was net

496   heterotrophic with a higher degree of heterotrophy at station TYR (NCP were -1.9, -0.2, -0.8

497   µmol O$_2$ L^{-1} d^{-1} at TYR, ION and FAST, respectively, as measured in the controls from seawater

498   sampled at t0). CR and GPP rates were respectively the highest and the lowest at station TYR

499   compared to the other two stations. Finally, BP rates were the highest at station FAST (35.8 ng C

500   L^{-1} h^{-1}), intermediate at ION (26.1 ng C L^{-1} h^{-1}) and the lowest at TYR (21.3 ng C L^{-1} h^{-1}).

3.2. Changes in biological stocks

502   DOC concentrations showed a general positive trend during the three experiments and a

503   large variability between duplicates (Fig. 2). This variability appeared as soon as 1 h after dust

504   seeding (t1h) while the range of variation at t0 (before dust seeding) was rather moderate

505   (difference between minimal and maximal values in all tanks of 1.3, 6.2 and 4.3 µmol C L^{-1} at

506   station TYR, ION and FAST, respectively). As a consequence of this variability, no clear impact

507   of dust seeding (D) could be highlighted at station TYR and FAST. Indeed, DOC concentrations

508   in the two duplicates (D1 and D2) were higher than values in the controls (C1 and C2) in only

Deleted: 2020

Formatted: English (US)

Deleted: increasing

511 33% of the samples along the experiments (after dust seeding). In contrast, at station ION, DOC

512 concentrations appeared impacted by dust seeding as higher concentrations were almost

513 systematically (83% of the time after dust seeding) measured for this treatment as compared to

514 control tanks at the same time. At all stations, this impact was somewhat exacerbated under

515 conditions of temperature and pH projected for 2100 (G1 and G2) as DOC concentrations were

516 almost all the time higher in these tanks than in control tanks (83 - 100% of the samples after

517 dust seeding, depending on the station).

518 Total hydrolysable carbohydrates and amino acids concentrations along the three

519 experiments are shown in Fig. S2. TCHO concentrations were quite variable between tanks

520 before dust seeding (t0; 649 - 954, 569 - 660 and 600 - 744 nmol L^{-1} at station TYR, ION and

521 FAST, respectively) and no visible impact of the treatments were visible at station TYR (TCHO

522 tended to decrease everywhere). In contrast, at station ION and FAST, values in dust amended

523 tanks increased and appeared higher than in control tanks towards the end of the experiments

524 although the large variability between duplicates tended to mask this potential effect. An impact

525 of dust seeding was much clearer for TAA concentrations that showed larger increases

526 throughout the three experiments in tanks D1 and D2 as compared to control tanks, this effect

527 being exacerbated for warmer and acidified tanks (G1 and G2). The ratio between TAA and

528 DOC concentrations (Fig. 2) showed positive trends in tanks D and G during all three

529 experiments with a clear distinction between treatments at the end of the experiments (G > D >

530 C). The strongest increase was observed at station FAST in tanks G where final TAA/DOC ratios

531 were above 3%.

532 Particulate organic carbon (POC) concentrations strongly decreased at all stations

533 between t-12h and t0, this decrease being the largest at station TYR where concentrations

| Deleted: increasing |

| Deleted: values |

21

536 dropped from 25.7 to 9.6 - 13.2 µmol C L^{-1} (Fig. 3). After dust seeding, POC concentrations did

537 not show clear temporal trends for the three experiments although a slight general increase could

538 be observed at station FAST. Furthermore, no impact of dust seeding and warming/acidification

539 could be observed on POC dynamics. While concentrations of transparent exopolymer particles

540 (TEP-C) were rather constant through time in control tanks at the three stations, a large increase

541 was observed in dust-amended tanks (D and G) with TEP-C reaching values up to ~2 µmol C L^{-1}

542 in tank G1 at station TYR after 24 h (i.e. ~17% of POC concentration, Fig. 3). In all cases except

543 for tank G2 at station ION, TEP-C further decreased towards the end of the experiments although

544 concentrations remained well above those observed in the controls. As the variability between

545 duplicated tanks G was rather high, no impact of warming/acidification on TEP dynamics could

546 be highlighted at the three stations.

3.3. Changes in metabolic rates

548 ^{14}C-based particulate production rates as measured during the different time intervals at

549 the three stations were low in control tanks (maximal total particulate production of 0.34 µg L^{-1}

550 h^{-1} at station FAST) and did not show any particular temporal dynamics (Fig. 4). In these tanks,

551 the vast majority of particulate production was attributed to cells above 2 µm (65 - 89%). The

552 percentage of extracellular release (%PER) was overall maximal at station TYR and minimal at

553 station FAST with a tendency to decrease with time at the three stations although large variations

554 were observed between duplicates.

555 Dust addition alone did not have any clear positive impact on all ^{14}C-based rates at

556 station TYR, with even an observable decrease in production rates from larger cells (> 2 µm)

557 compared to the controls. In contrast, at this station, dust seeding under warmer and acidified

558 conditions (tanks G) had a positive effect on particulate production rates, this effect being

Deleted: for this parameter

22

560 particularly visible for cells < 2 μm and to a lesser extent on dissolved production with a general

561 decrease of %PER. An important discrepancy between the duplicates of treatment G was

562 observable at the end of the experiment with much larger rates measured in tank G2.

563   In contrast to station TYR, an enhancement effect of dust addition was clearly visible at

564 station ION where all rates increased towards the end of this experiment reaching a maximal

565 total particulate production of 0.6 - 0.7 μg L^{-1} h^{-1} in tanks D1 and D2. Since this positive effect

566 was similar between small and larger cells, dust addition alone had no effect on the partitioning

567 of production at this station, with cells > 2 μm representing ~80% of total production. Although

568 being also positively impacted and increasing with time, dissolved production appeared less

569 sensitive than particulate production leading to an overall decrease of %PER at station ION

570 following dust addition. These positive impacts of dust seeding on ^{14}C-based particulate

571 production rates were even more visible at this station under warmer and acidified conditions

572 (tanks G) with maximal rates more than doubled compared to those measured under present

573 conditions of temperature and pH (1.5 - 1.6 μg L^{-1} h^{-1}). Dust seeding under warmer and acidified

574 conditions had a slight impact on the partitioning of particulate production at station ION with

575 smaller cells benefiting the most from these conditions. %PER remained between 20 and 30%.

576   At station FAST, similarly to station ION, total particulate production rates were clearly

577 enhanced by dust addition (tanks D) reaching maximal values during the incubation time interval

578 t48 - 56h. No clear increase was observed for total particulate production on the next incubation

579 (t96 - 120h) while production rates of cells larger than 2 μm increased and rates of smaller cells

580 decreased. However, in contrast to station ION, there was much less impact of

581 warming/acidification on all measured rates at station FAST although rates measured on smaller

582 cells (< 2 μm) did not decrease at the end of the experiment as observed under present

23

Deleted: this

Deleted: this

Deleted: at FAST, in contrast to station ION

586   environmental conditions. %PER under both present conditions of temperature and pH (tanks D)

587   decreased during this experiment reaching values lower than in the controls and in tanks G.

588   The initial enrichment of the tanks in ^{13}C-bicarbonate led to an increase in the ^{13}C

589   signature of dissolved inorganic carbon (δ^{13}C-C_T) of above 300‰, with generally lower values

590   measured in warmer and acidified tanks (G; Fig. S3). After this initial enrichment, δ^{13}C-C_T levels

591   decreased linearly in all tanks. At stations TYR and ION, the isotopic signature of dissolved

592   organic carbon (δ^{13}C-DOC; Fig. S3) increased with time, although these increases were rather

593   low and limited to ~ 4‰ over the course of the experiments. In contrast to station TYR, at ION,

594   an enhanced incorporation of ^{13}C into DOC was visible after 24 h in tanks D and G in

595   comparison to control tanks. A similar observation was done at station FAST, especially at the

596   end of the experiment, although much more variability was observed at this station.

597   The incorporation of ^{13}C into particulate organic carbon (δ^{13}C-POC) is shown in Fig. 5.

598   At all stations, δ^{13}C-POC increased with time but reached lower enrichment levels at station

599   TYR as compared to ION and FAST. At station TYR, incorporation rates appeared smaller in

600   dust-amended tanks under present environmental conditions (tanks D). As for ^{14}C-based

601   production rates, an important discrepancy was observed between duplicates under future

602   conditions of temperature and pH (tanks G) with much higher final δ^{13}C-POC at the end of the

603   experiment in tank G2. At station ION, enrichment levels obtained at the end of the experiment

604   were more important in dust-amended tanks reaching maximal levels of 73‰ in tank G2 at t72h.

605   This enhancement effect was even more visible at station FAST with maximal enrichment levels

606   of 146‰ (tank D2 at t96h). Since no sampling occurred at t72h, these enrichment levels cannot

607   be directly compared to what was measured at station TYR and ION. However, by interpolating

Deleted: o

Deleted: this

24

610 values at t72h assuming a linear increase between these time intervals, enrichment levels

611 appeared similar although slightly higher for tanks D between station ION and FAST.

612   NCP rates as measured using the O_2 light-dark method showed that, under control

613 conditions, the communities remained the vast majority of the time throughout the three

614 experiments in a net heterotrophic state (NCP < 0; Fig. 6). This was especially true at station

615 TYR where the lowest NCP rates were measured. At this station, dust addition whether under

616 present or future conditions of temperature and pH did not switch the community towards net

617 autotrophy but even drove the community towards a stronger heterotrophy. This was related to

618 the fact that while gross primary production rates were not positively impacted, community

619 respiration increased in tanks D and G. At station ION, dust addition alone (tanks D) led to a

620 switch from net heterotrophy to net autotrophy after two days of incubation due to a stronger

621 positive effect of dust on GPP than on CR. Under future environmental conditions (tanks G), the

622 same observation was made with higher NCP and GPP rates than in tanks D. CR rates reacted

623 quickly to these forcing factors in tanks G and initially (first incubation) drove the community

624 towards a much stronger heterotrophy as compared to the other tanks. Finally, at station FAST,

625 similarly to what was observed at ION, the community became autotrophic after two days of

626 incubation in dust amended tanks as, although both GPP and CR were positively impacted by

627 dust addition, this impact was less important for CR. Warming and acidification had a limiting

628 impact on this enhancement, with a lower final NCP in tanks G compared to tanks D, a

629 difference that can be related to an absence of effects of these environmental stressors on GPP

630 while CR clearly increased at higher temperature and lower pH.

631   While BP remained constant or gradually increased in control tanks depending on the

632 station, a clear and quick fertilization effect was observable following dust addition (treatment D

25

633 and G) at all stations (Fig. 7). At station TYR, BP rates sharply increased to reach maximal

634 values at t24h, with an even stronger increase observed under warmer and acidified conditions

635 (tanks G). After this initial increase, rates slightly decreased towards the end of the experiment.

636 This fertilization effect appeared less important at station ION where lower maximal rates were

637 obtained after 24 h as compared to station TYR. Nevertheless, the same observations can be

638 made, namely, 1) higher rates were measured under future temperature and pH levels and 2) after

639 this initial sharp increase, rates gradually decreased towards the end of the experiment especially

640 in tanks G. At station FAST, a much stronger effect of warming/acidification was observed with

641 an important increase of BP in tanks G until 24 or 48 h post-seeding, depending on the duplicate.

642 A sharp decline was observed for this treatment until the end of the experiment although rates

643 remained higher than those measured in tanks C and D. The impact of dust addition under

644 present environmental conditions (tanks D) was somehow more limited than at the other stations

645 with a gradual increase until t72h with maximal rates ~ 40 - 100% higher than rates measured in

646 the controls. However, BP increased exponentially between t0 and t12h in all tanks including

647 controls, and in all experiments (Table 2). The growth rate of BP (μ_{BP}) in control tanks was the

648 highest at TYR, intermediate at ION and the lowest at FAST. μ_{BP} increased significantly in all

649 dust amended tanks compared to controls. Under future environmental scenarios, μ_{BP} tended to

650 increase compared to treatment D but with a variable relative change (Table 2).

651   BGE increased in dust amended tanks under present environmental conditions (treatment

652 D) at TYR and ION, while no changes were detectable at station FAST due to a strong

653 discrepancy between control duplicates and overall higher BGE at this station in the controls

654 (Table 3). In contrast, warming and acidification exerted the strongest effect at station FAST

655 with a doubling of BGE between treatment G and D. Although an increase in BGE was also

26

656 observed at the two other stations in treatment G as compared to present environmental

657 conditions (treatment D), this increase was more limited (ca. 1 to 1.4-fold increase).

658 The alkaline phosphatase Vm (AP Vm) increased in all experiments after dust seeding,

659 with amplified effects in G treatments (Fig. S4). Note that AP Vm increased also in the controls

660 at TYR and FAST. In contrast, leucine aminopeptidase Vm (LAP vm) showed succession of

661 peaks instead of a continuously increase (Fig. S4). It was higher in dust alone treatment (D) as

662 compared to the controls at TYR and FAST. A larger variability between duplicates at ION

663 prevents such an observation. At all stations, maximum velocities were measured under future

664 environmental conditions (G). Vm being possibly influenced by enzyme synthesis but also by the

665 number of cells inducing such enzymes, we computed also specific AP Vm per heterotrophic

666 bacterial cell (Fig. 7). Specific AP Vm slightly increased during all experiments in controls and

667 dust-amended tanks (D) with no visible differences between these treatments, a clear over-

668 expression of this enzyme was observed under warmer and more acidified conditions (treatment

669 G) especially at station FAST where velocities were enhanced by a ~8-fold at t96h.

3.4. Inorganic and organic material export

671 Both total mass and organic matter fluxes, as measured from analyses of the sediment

672 traps at the end of each experiment, were extremely low under control conditions (Fig. 8). Only

673 less than 30% of the dust introduced at the surface of the tanks were recovered at the end of the

674 experiment (3 or 4 days after) in the sediment traps with TYR>ION>FAST. The composition of

675 the exported material was quite similar for each experiment with no significant difference

676 between D and G treatments with 3-5% opal, 4% organic matter, 35-36% $CaCO_3$ and 48-54%

677 lithogenic (Fig. S5). Additions of dust in tanks D and G led to a strong increase in both fluxes

678 with a large variability between the duplicates of treatment D at ION. No clear changes between

680   tanks maintained under present and future conditions of temperature and pH could be

681   highlighted.

4. Discussion

4.1. Initial conditions of the tested waters and evolution in controls

As discussed in details in the companion paper from Gazeau et al. (2021), the three sampling stations were typical of stratified (mixed layer depth of 10-20 m) oligotrophic conditions encountered in the open Mediterranean Sea in late spring / early summer. Briefly, the low NO_x:DIP ratios nutrient concentrations suggest that communities found at the three stations experienced N and P co-limitation at the start of the experiments. The composition of the smaller size phytoplankton communities differed substantially, with autotrophic nano-eukaryotes dominating at stations TYR and ION and a larger contribution from autotrophic pico-eukaryotes and Cyanobacteria at station FAST. The observed low total chlorophyll a concentrations and the small contribution of large phytoplankton cells at the start of the three experiments are characteristic of LNLC areas in general, and of surface Mediterranean waters in late spring and summer (Siokou-Frangou et al., 2010). DOC concentrations at the start of the experiments were in the same range (60 - 75 μmol C L^{-1}) as those measured from samples collected in surface waters using clean sampling procedures (Van Wambeke et al., 2021), revealing no contamination issues from our sampling device. TAA concentrations as measured in the tanks at t0 were also consistent with measurements from surface water samples (Van Wambeke et al., 2021) with an average across stations and treatments of 254 ± 36 nmol L^{-1} (Fig. S2). In contrast, TCHO appeared higher at t0 (average across stations and treatments of 681 ± 98 nmol L^{-1}) than concentrations based on clean *in situ* sampling (average of 595 ± 43 nmol L^{-1}; Van Wambeke et al., 2021). The decrease in POC concentrations between pumping (t-12h) and t0 for the three

709 experiments, especially at station TYR (likely linked to higher initial concentrations), was likely

710 a consequence of sedimentation of senescent cells and/or fecal pellets in our experimental

711 systems, which are designed to evaluate the export of matter thanks to their conical shape. TEP

712 concentrations were not quantified at t-12h and therefore there is no possibility to evaluate if

713 sedimentation of these particles occurred before t0 in our tanks. At t0, larger and more abundant

714 TEP were measured at station TYR compared to the two other stations (data not shown).

715   As a consequence of a very low availability in inorganic nutrients, TChl$a$ and ^{14}C-based

716 production rates were very low, all typical of oligotrophic conditions. Nano- and micro-

717 phytoplanktonic cells (> 2 μm) contributed most of the ^{14}C-based particulate production (~ 80%),

718 as found also on several on-deck incubations at the three stations (on average 73 ± 6%; Marañón

719 et al., 2021). %PER values were also very similar to those measured during these on-deck

720 incubations (~ 40-45%; see Marañón et al., 2021). This suggests no significant impact of our

721 experimental protocol on rates and partitioning of ^{14}C-based production rates (i.e. sampling from

722 the continuous seawater supply, delay of 12 h before initial measurements, artificial light etc.).

723 The low values of chlorophyll stocks as well as of ^{14}C-based production rates are consistent with

724 previous estimates based on direct measurements, satellite observations and modelling

725 approaches in the same areas in late spring / early summer (e.g. Bosc et al., 2004; Lazzari et al.,

726 2016; Moutin and Raimbault, 2002).

727   The metabolic balance was in favor of net heterotrophy at all stations at the start of the

728 experiments (NCP < 0). Net heterotrophy in the open Mediterranean sea at this period of the year

729 has been reported by Regaudie-de-Gioux et al. (2009) and Christaki et al. (2011) in agreement

730 with our measurements at t0 in control tanks (Table 1). The lowest NCP and the highest CR rates

731 were measured at station TYR, suggesting that the autotrophic plankton community was not very

Deleted: leading to a larger contribution of TEP carbon content (TEP-C) to POC concentrations (Fig. 3)

Formatted: English (US)

Deleted: 0

Formatted: English (US)

Formatted: English (US)

Deleted: 0

Formatted: English (US)

Formatted: English (US)

Formatted: English (US)

Formatted: English (US)

Formatted: English (US)

Formatted: English (US)

Formatted: English (US)

736 active at this station. This was confirmed by the ^{14}C-based particulate production rates, which

737 were about half the ones measured at the other two stations. The community at TYR was most

738 likely relying on regenerated nutrients, as shown by the highest levels of ammonium (NH_4^+)

739 measured at the start of this experiment (Gazeau et al., 2021). As discussed in Guieu et al.

740 (2020a), a dust deposition event took place several days before the arrival of the vessel in this

741 area, likely on May 10-12. This dust event was confirmed by inventory of particulate aluminium

742 in the water column at several stations of the Tyrrhenian Sea including TYR, 6 to 9 d after the

743 event (Bressac et al., 2021). This dust deposition likely stimulated phytoplankton growth and

744 POC accumulation shortly after the deposition and consequently increased the abundance of

745 herbivorous grazers (copepods) and attracted carnivorous species (Feliú et al., 2020),

746 subsequently driving the community towards a net heterotrophic state that characterized the

747 initial condition of the experiment at this station. The favorable conditions for BP growth at TYR

748 were also confirmed by the highest μ_{BP} growth rates obtained among the three experiments

749 (Table 2; 0.06 - 0.07 h^{-1}) in controls tanks.

750   The two other stations, although both also showing a slight net heterotrophic state, were

751 clearly different from each other in terms of initial biological stocks and metabolic rates. Indeed,

752 whereas TChl*a* and abundances of pico- and nano-autotrophic cells (flow cytometry counts;

753 Gazeau et al., 2021) were higher at FAST compared to ION, the autotrophic community was not

754 more efficient at fixing carbon at FAST, as shown by similar initial ^{14}C-based production rates.

755 In contrast, both heterotrophic prokaryotic abundances and BP were much higher at station

756 FAST as compared to ION, leading to initial higher CR and lower NCP. At ION, the initial NCP

757 closer to metabolic balance further suggests a tight coupling between heterotrophic prokaryotes

758 and phytoplankton at this station, as discussed by Dinasquet et al. (2021).

31

766 For most of the chemical and biological stocks (e.g. nutrients, pigments etc.) presented in

767 Gazeau et al. (2021), no major changes took place during the three experiments under control

768 conditions. Here, we further show that DOC, POC as well as TEP concentrations did not exhibit

769 strong changes during the experiments. For DOC, large variability between the duplicates (C1

770 and C2) potentially masked an increase towards the end of the experiments. The same holds true

771 for autotrophic metabolic rates, as ^{14}C-based particulate production rates showed no marked

772 variations during the three experiments, although a slight increase was visible at FAST until

773 t48h. The communities at the three stations remained heterotrophic under the nutrient-limited

774 conditions in the controls. However, heterotrophic prokaryotes probably benefited from initial

775 inputs of available organic matter issued from other stressed eukaryotic organisms and/or POC

776 decay between t-12h and t0, which could be due to both sedimentation and degradation. This was

777 reflected in the progressive increase of BP, their variable initial growth rates (μ_{BP} ranged from

778 0.02 to 0.06 h^{-1} in control tanks according to the experiment) as well as increasing TAA/DOC

779 ratios at the three stations. Finally, an initial increase of BP during incubations is generally

780 described and classically attributed to a bottle effect, which favours large, fast-growing bacteria

781 and often induces mortality of some phytoplankton cells (Calvo-Díaz et al., 2011; Ferguson et

782 al., 1984; Zobell and Anderson, 1936).

783 ## 4.2. Impact of dust addition under present environmental

784 ## conditions

785 The addition of nitrogen and phosphorus in the experimental tanks through dust seeding

786 (+ 11 to + 11.6 μmol L^{-1} and + 22 to + 30.8 nmol L^{-1} for NO$_x$ and DIP, respectively, in dust

787 enriched, i.e. D1 and D2, versus controls; Gazeau et al., 2021) had very contrasting impacts on

32

790 the metabolism of the communities, depending on the station. At TYR, surprisingly, the relieving

791 of nutrient (N, P) limitation had a negative impact on ^{13}C incorporation as well as on both

792 particulate and dissolved ^{14}C-based production rates (as seen by the relative changes compared to

793 the control presented in Fig. 9). These observations are fully corroborated by the observed

794 relative decrease in GPP in these tanks (D1 and D2) relative to controls and by the negative

795 impact of dust-addition on TChl*a* concentrations as discussed by Gazeau et al. (2021). Integrated

796 ^{14}C-incorporation rates converted to P (using a C:P molar ratio of 245:1 determined in the

797 particulate organic matter in surface waters of the Northwestern Mediterranean Sea during

798 stratification; Tanaka et al., 2011) showed that phytoplankton P requirements in treatment D (~2

799 nmol P L^{-1}) were much lower than the release of DIP through dust addition at station TYR (+

800 20.4 to + 24.6 nmol P L^{-1}; Gazeau et al., 2020). This suggests that the observed strong decrease

801 of DIP at TYR following dust addition was due to an utilization by the heterotrophic

802 compartment. Indeed, in contrast to the autotrophic compartment, both heterotrophic prokaryotic

803 abundances (Gazeau et al., 2021) and BP (this study, Fig. 9) showed that heterotrophic

804 prokaryotes reacted quickly and strongly to the increase in DIP availability. Integrated BP

805 increased by almost 400% in tanks D1 and D2 as compared to controls (Fig. 9). Such relative

806 increases of BP surpassing by far the observed relative increases of CR suggest a much more

807 efficient utilization of resources by heterotrophic prokaryotes in this treatment (i.e. BGE

808 increased by 200% as compared to the controls; Fig. 9). As such, at TYR, the addition of dust

809 drove the community to an even more heterotrophic state. Such absence of response of the

810 autotrophic community despite the input of new N and P from simulated wet deposition was

811 never observed in dust enrichment experiments performed in the Mediterranean Sea (Guieu and

812 Ridame, 2020). To the best of our knowledge, it is the first time that a negative effect of dust

33

818   addition is experimentally demonstrated on the metabolic balance. The apparent utilization of

819   nutrients, especially DIP (Gazeau et al., 2021), by heterotrophic prokaryotes was extremely fast,

820   starting right after dust addition and driving DIP concentrations back to control levels at the end

821   of the experiment (t72h). While heterotrophic prokaryotic abundances increased until the end of

822   the experiment, BP rates increased exponentially during the first 24h, and then BP reached a

823   plateau. Heterotrophic prokaryotes appeared limited by nutritive resources although DIP

824   concentrations were not yet back to their initial level and no relative increase of the AP Vm per

825   cell compared to the control was observed in these tanks. Independent nutrient experiments

826   showed a direct stimulation of BP in the dark after addition of DIP (Van Wambeke et al., 2021),

827   suggesting a great competition with phytoplankton for DIP utilization at TYR. After 24 h,

828   abundances of heterotrophic prokaryotes continued to increase while BP stabilized, suggesting a

829   less extent of lysis and viral control than in the other experiments (abundances of heterotrophic

830   nanoflagellates decreased; Dinasquet et al., 2021). This limitation of BP was potentially a

831   consequence of relatively less available access to labile DOC sources, as ^{14}C-based production

832   rates decreased relative to the controls at t24h and t48h although BP increased by 200 - 800%.

833   The very tight coupling between phytoplankton and bacteria at all stations investigated was

834   further confirmed by the absence of an important ^{13}C incorporation into DOC (Fig. S3).

835   At stations ION and FAST, in contrast to TYR, both the autotrophic and heterotrophic

836   community benefited from dust addition relative to the controls (Fig. 9). Interestingly, while the

837   relative increase in integrated autotrophic processes (GPP and all ^{14}C-based production rates)

838   was more important at FAST than at ION, the opposite was observed for BP. Estimated BGE

839   values even suggest an absence of response to dust addition at station FAST compared to the

840   controls. The different (relative) responses of BP at the two stations could be partly explained by

843   the dynamics of BP in the control tanks as no clear pattern could be observed at ION while a

844   continuous increase was observed at FAST. As shown by Gazeau et al. (2021), at FAST,

845   abundances of heterotrophic prokaryotes were much higher at the start of the experiment, further

846   increased until t48h and then declined until the end of the experiment.

847   We can rule out a potential limitation of BP from DIP availability at station FAST as DIP

848   levels remained much higher in tanks D than in the controls (Gazeau et al., 2021). Furthermore,

849   the amount of maximum DIP reached before its decline compared to TYR and ION showed a

850   less important direct DIP uptake, suggesting that communities were not as much P limited at

851   FAST compared to the other stations at the start of the experiment. Finally, no increase of

852   specific AP Vm was observed in these tanks as compared to the controls (Fig. 7), suggesting no

853   particular additional needs for AP synthesis per unit cell following dust addition. A potential

854   explanation resides in the competition between heterotrophic bacteria and phytoplankton for DIP

855   utilization. At station ION, P requirements of the autotrophic community were low compared to

856   the initial input of DIP following dust seeding (~9 nmol P L^{-1} as compared to an input of + 22 to

857   + 23.3 nmol P L^{-1}; Gazeau et al., 2021). In contrast, at FAST, the autotrophic community

858   consumed a much larger proportion of the initial DIP input (~25 nmol P L^{-1} as compared to an

859   input of 30.8 - 31.3 nmol P L^{-1}) and phytoplankton appeared as a winner for the utilization of

860   DIP towards the end of the experiment at this station. It seems that heterotrophic bacteria and

861   phytoplankton were more in balance and less stressed at the start of the experiment at FAST, i.e.

862   phytoplankton abundances showed no decrease between t-12h and t0 and BP did not increase as

863   much as during the other two experiments, suggesting a strong predation pressure (μ_{BP} was the

864   lowest of the three experiments: ca. 0.02 h^{-1} in the controls).

869   The explanation for the observed differential responses of the autotrophic community at

870   the two stations (FAST > ION) is not evident and further complicated by the fact that the

871   sampling strategy differed between the two stations (i.e. no sampling at t72h, replaced by a

872   sampling at t96h). It is however unlikely that this different sampling strategy was responsible for

873   the different changes in computed integrated autotrophic rates at the two stations. As a maximal

874   increase in nano-eukaryote abundance was observed at t72h at FAST (followed by a drastic

875   reduction at t96h; Gazeau et al., 2021), excluding this sampling point in the calculation of

876   autotrophic metabolic rates would most likely have led to an underestimation of these rates rather

877   than an overestimation. Furthermore, a similar partitioning of ^{14}C-based production rates

878   throughout the two experiments did not provide clear insights on which size-group benefited the

879   most at station FAST compared to ION. Two non-exclusive explanations could be proposed: (1)

880   as mentioned above, a less important immediate consumption of DIP by heterotrophic bacteria

881   leading to a higher availability of new DIP for phytoplankton growth at FAST (+ 31 vs + 22 to +

882   23 nmol L^{-1} at FAST and ION, respectively; Gazeau et al., 2021) along with (2) the presence of a

883   potentially more active community at the start of the experiment at FAST with a much higher

884   contribution from smaller cells (i.e. pico-eukaryotes, *Synechococcus*; Gazeau et al., 2021) that

885   are well known to be better competitors for new nutrients (e.g. Moutin et al., 2002) and that were

886   less stressed at the start of the experiments.

887   During both experiments at ION and FAST, communities switched from net heterotrophy

888   to net autotrophy between 48 and 72 h following dust addition (Fig. 6), leading to a positive

889   integrated NCP at both stations (Fig. 9). This is an important observation since, to the best of our

890   knowledge, the present study constitutes the first investigation of the community metabolism

891   response to dust addition. However, it is important to discuss the timing of such a switch in

36

896 community metabolism. Since heterotrophic prokaryotes reacted faster than autotrophs to the

897 relief of nutrient (N, P) limitation (i.e. BP already increased by 150-500% at t24 h, while ^{14}C-

898 based production rates increased only after 48-72 h), NCP was first lower (and negative) in the

899 dust-amended tanks as compared to the controls. Marañón et al. (2010) and Pulido-Villena

900 (2008, 2014) have already reported on a much faster response of the heterotrophic prokaryote

901 community to dust enrichment in the central Atlantic Ocean and Mediterranean Sea,

902 respectively. As DIP concentrations at the completion of their 48 h incubations did not differ

903 from that in the controls, it is unlikely that primary production rates and consequently NCP

904 would have further increased. In contrast, during our experiments, DIP concentrations in dust-

905 amended tanks (D) reached initial levels only after 72 h at TYR and ION and remained far above

906 ambient levels at FAST until the end of the experiment (t96h). During the PEACETIME cruise,

907 high frequency sampling of CTD casts allowed following the evolution of biogeochemical

908 properties and fluxes before and after wet dust deposition that took place in the area around

909 FAST on June 3-5 (Van Wambeke et al., 2020). As in our experiment, a rapid increase in BP was

910 responsible for the observed *in situ* decline in DIP concentrations in the mixed layer following

911 the rain with no detectable changes in primary production (Van Wambeke et al., 2020). The

912 intensity of the wet deposition event that was simulated during our experiments was, by far,

913 higher, but still representative of a realistic scenario (Bonnet and Guieu, 2006; Loÿe-Pilot and

914 Martin, 1996; Ternon et al., 2010).

915   The most intriguing result concerning the export of inorganic and organic matter is that

916 these fluxes were maximal at the end of the experiment at TYR in the dust-amended tanks

917 despite the fact that ^{14}C-based production was relatively low and not enhanced by dust addition.

918 Based on previous studies (Bressac et al., 2014; Louis et al., 2017; Ternon et al., 2010), organic

922 matter export was most likely mainly due to the formation of organic-mineral aggregates

923 triggered by the introduced lithogenic particles (referred thereafter to as POC_{litho}). Indeed, Louis

924 et al. (2017) showed that such an aggregation process occurs within 1 h after dust deposition.

925 These authors further demonstrated the key role of TEP as the conversion of dissolved organic

926 matter (DOM) to POC was mediated by TEP formation/aggregation activated by the introduction

927 of dust. As TEP concentrations were only measured on two occasions after seeding with the first

928 measurement occuring at t24h,), it prevents studying in detail the dynamics of these particles.

929 Nevertheless, it is very likely that the sharp decrease of TEP-C (Fig. 3) between t24h and t72h

930 was related to POC_{litho} export. The coefficient linking POC_{litho} to $Litho_{flux}$ (i.e. the mass of

931 sedimented particles) measured here (0.02) is consistent with values reported for other

932 experiments conducted in the Mediterranean Sea (Louis et al., 2017).

933 Even though ^{14}C-based production rates were enhanced in the dust-amended tanks at

934 stations ION and FAST, the amount of POC exported at the end of these experiments remained

935 lower than at TYR, with fluxes ~ 10-20 mg C m^{-2} d^{-1}.

936 The recovery of the introduced dust (traced by the lithogenic mass recovered in the traps)

937 was low (27% at TYR, ~20% at ION and 13-19% at FAST) reflecting that a majority of the dust

938 particles (the smaller ones that are the most abundant according to the particle size distribution of

939 the dust) still remained in the tanks after 3 or 4 days following dust addition. This has been

940 already observed in pelagic mesocosms (Bressac et al., 2012) as those small particles can

941 aggregate to organic matter and eventually sink. The higher export efficiency observed

942 (TYR>ION>FAST) is likely linked to the higher initial abundance and higher production of

943 TEPs during the experiment (Fig. 3). At TYR, impacted by a strong dust event several days

944 before the experiment started (see above), the likely stimulation of the autotrophs after this *in*

Formatted: English (US)

Formatted: English (US)

Deleted: abundances

Deleted: data not shown

Formatted: English (US)

Formatted: English (US)

Formatted: English (US)

Formatted: Font: Not Italic

Formatted: English (US)

Formatted: Font: Not Italic

Deleted: It must be stressed that not all the lithogenic material introduced in the tanks was recovered after 4 (and 5) days, with the highest percentage (~ 30%) being found at TYR, indicating that the tested waters at this station had a better capacity to aggregate dust. This efficiency to export POC_{litho} more rapidly at TYR compared to ION and FAST was likely due to the age and quantity of dissolved organic matter present at the time of the seeding (Bressac and Guieu, 2013)…

Formatted: English (US)

38

956 *situ* event should have been followed by the production of a fresh and abundant DOM,

957 comparable to the "post-bloom situation" in Bressac and Guieu (2013).

4.3. Impact of dust addition under future environmental

959 conditions

960   Warming and/or acidification had a clear impact on most evaluated stocks and metabolic

961 rates. Gazeau et al. (2021) have already discussed temperature/pH mediated changes in nutrient

962 uptake rates and autotrophic community composition in these experiments. Briefly, they showed

963 that warming and acidification did not have any detectable impact on the release of nutrients

964 from atmospheric particles. Furthermore, these external drivers did not drastically modify the

965 composition of the autotrophic assemblage with all groups benefiting from warmer and acidified

966 conditions. Here, we showed that the difference in the response of plankton community

967 metabolism to dust addition under present and future conditions of temperature and pH was

968 highly dependent on the sampling station (Fig. 9). At all stations, ^{14}C-based particulate

969 production rates were enhanced under future conditions as compared to those measured under

970 present environmental conditions (treatment D) although this pattern was not observed for ^{13}C

971 incorporation into POC at stations ION and FAST. At ION, no differences could be detected and

972 at FAST an even lower ^{13}C-enrichment was measured at the end of the experiment. These

973 contrasting patterns between ^{14}C-uptake rates and ^{13}C-enrichment of POC are likely explained by

974 the fact that the latter covered the whole experimental period (including dark periods) and

975 represents net community carbon production while ^{14}C-based rates were measured over 8 h

976 incubations in the light, providing an estimate in between gross and net carbon production.

981   Similarly, the heterotrophic compartment was more stimulated, as BP rates increased

982 strongly at all stations under future conditions compared to treatment D. The relatively smaller

983 increase in CR rates, compared to BP, leading to higher BGE suggests a better utilization of

984 resources by heterotrophic prokaryotes under future environmental conditions. Overall, CR was

985 more impacted than GPP, with the consequence that all integrated NCP rates decreased under

986 future environmental conditions compared to present conditions (treatment D). At station TYR,

987 as discussed previously, dust addition under present conditions did not lead to a switch from net

988 heterotrophy to net autotrophy. This pattern was even more obvious under warmer/acidified

989 conditions, with a larger decrease in integrated NCP at this station. The decrease of integrated

990 NCP at station FAST relative to controls, as well as the smaller increase of all ^{14}C-based

991 production rates relative to those observed at station ION must be taken with caution. As already

992 discussed, the fact that for these processes (O_2 metabolism and ^{14}C-incorporation), no samples

993 were taken at FAST at t72h when maximal cell abundances were recorded for all autotrophic

994 groups (pico- and nano-eukaryotes, autotrophic bacteria) must have artificially led to an

995 underestimation of these integrated metabolic rates. The question of the timing appeared even

996 more preponderant under warmer/acidified conditions, especially at station FAST, where the

997 very important increase in BP led to a full consumption of DIP before t48h (Gazeau et al., 2021)

998 and drove the community towards a strong heterotrophy. The metabolic balance further switched

999 to a slight autotrophy at t72h when heterotrophic bacterial activity appeared limited by nutrient

1000 availability.

1001   Both elevated partial pressure of CO_2 ($p$$CO_2$) and warming are major global change

1002 stressors impacting marine communities. Elevated $p$$CO_2$ may directly facilitate oceanic primary

1003 production through enhanced photosynthesis (Hein and Sand-Jensen, 1997; Riebesell et al.,

2007), although the effects appear to be species- and even strain-specific (e.g. Langer et al.,

2009). Warming affects organisms by enhancing their metabolic rates (Brown et al., 2004;

Gillooly et al., 2001). Although recent studies suggest large differences in temperature sensitivity

between phytoplankton taxa (Chen and Laws, 2017) and no significant overall difference

between algae and protozoa (Wang et al., 2019), mineralization rates are usually believed to be

more impacted by warming than primary production rates, potentially leading to a decline in net

oceanic carbon fixation (Boscolo-Galazzo et al., 2018; Garcia-Corral et al., 2017; Lopez-Urrutia

and Moran, 2007; Regaudie-de-Gioux and Duarte, 2012) and carbon export efficiency (Cael et

al., 2017; Cael and Follows, 2016). Overall, our experimental set-up did not allow discriminating

warming from acidification effects, precluding an evaluation of their potential individual

impacts. Nevertheless, we could speculate to which extent a 3 ºC warming and a doubling of

CO_2 can explain some of the observed differences between D and G (for instance, a 2-fold

increase in ^{14}C-based production rates at ION). For photosynthesis, meta-analysis studies

indicate minor effects of $p$$CO_2$ on most investigated species (Kroeker et al., 2013; Mackey et al.,

2015). Recent studies show a strong, although species-dependent, temperature sensitivity of

phytoplankton growth (Chen and Laws, 2017; Wang et al., 2019), suggesting that a 3 ºC

warming could explain most of the increased carbon fixation in G compared to D. With respect

to NCP, our results are in line with the general view and suggest a weakening of the so-called

fertilization effect of atmospheric deposition in the coming decades.

In contrast, we did not observe an additional impact of future environmental conditions

on the export of organic matter after dust addition as, at each station, this export was of the same

order of magnitude for treatments D and G. This result is in agreement with the findings of a

similar experiment in coastal Mediterranean waters that considered only pH change (Louis et al.,

41

2017) but stands in contrast with the findings of Müren et al. (2005) who showed a clear

decrease in sedimentation following a 5 °C warming in the Baltic Sea. Only a few studies have

addressed the combined effect of both temperature and pH changes on aggregation processes and

export but none considered dust as the particulate phase. These studies, focused mainly on the

formation of TEP, were inconclusive on the impact of these combined factors (Passow and

Carlson, 2012, and references therein). The potential effect of warming and acidification on

biogenic carbon export was certainly, over the rather restricted duration of the experiments,

insignificant as compared to the large amount of carbon exported through the lithogenic pump.

Although a longer experimental period would likely be necessary to clearly support an impact of

future conditions on export, those changes occur on a long time scale that cannot be easily

mimicked by experimental approaches. Only *in situ* co-located observations (atmospheric flux

and export in sediment traps) over long temporal scales would be necessary to ascertain the

interactive effects of these stressors at the decadal time scale.

5. Conclusion

Although the three experiments were conducted under rather similar conditions in terms

of nutrient availability and chlorophyll stock of the tested seawater, contrasting responses were

observed following the simulation of a wet dust deposition event. Under present conditions of

temperature and pH, at the site where the community was the most heterotrophic (TYR), no

positive impact of new nutrients could be observed on autotrophs, while a fast and strong

response of heterotrophic bacteria drove the metabolic balance towards an even more

heterotrophic state. The situation was different at the two other stations where a more active

autotrophic community responded quickly to the relief in nutrient (N, P) limitation, driving the

community to an autotrophic state at the end of these experiments. In all tested waters, an overall faster response of the heterotrophic prokaryote community, as compared to the autotrophic community, was observed after new nutrients were released from dust. Phytoplankton could benefit from nutrient inputs, only if the amount released from dust was enough to sustain both the fast bacterial demand and the delayed one of phytoplankton. As our experimental protocol consisted in simulating a strong, although realistic, wet dust deposition, further work should explore at which flux a wet dust deposition triggers an enhancement of net community production and therefore increases the capacity of the surface oligotrophic ocean to sequester atmospheric CO_2. This question, of the utmost importance in particular for modelling purposes, should be answered through future similar experiments as the ones considered in our study but following a gradient approach of dust fluxes. As a consequence of a stronger sensitivity of heterotrophic prokaryotes to temperature and/or pH, the ongoing warming and acidification of the surface ocean will result in a decrease of the dust fertilization of phytoplankton in the coming decades and a weakening of the atmospheric CO_2 sequestration capacity of the surface oligotrophic ocean. The contrasting results obtained at the three stations during our study will need to be translated into process parameterization. The important dataset presented in this manuscript, covering a variety of tested waters, environmental stressors and responses, will allow such parameterization to be used in biogeochemical models coupled to ocean dynamics in order to depict the spatial and temporal dynamics of stocks and fluxes following dust deposition in surface oligotrophic waters.

Data availability

Underlying research data are being used by researcher participants of the PEACETIME campaign to prepare other manuscripts, and therefore data are not publicly acces- sible at the time of publication. Data will be accessible (http: //www.obs-vlfr.fr/proof/php/PEACETIME/peacetime.phpTS4, https://doi.org/10.17882/75747, Guieu et al., 2020b) once the special issue is completed (all papers should be published by fall 2021).

Author contributions

FG and CG designed and supervised the study. All authors participated in sample analyses. FG wrote the paper with contributions from all authors.

Financial support

Acknowledgments

References

Behrenfeld, M. J., O'Malley, R. T., Siegel, D. A., McClain, C. R., Sarmiento, J. L., Feldman, G. C., Milligan, A. J., Falkowski, P. G., Letelier, R. M. and Boss, E. S.: Climate-driven trends in contemporary ocean productivity, Nature, 444(7120), 752–755, 2006.

Benner, R. and Strom, M.: A critical evaluation of the analytical blank associated with DOC measurements by high-temperature catalytic oxidation, Mar. Chem., 41(1), 153–160, https://doi.org/10.1016/0304-4203(93)90113-3, 1993.

Bishop, J. K. B., Davis, R. E. and Sherman, J. T.: Robotic observations of dust storm enhancement of carbon biomass in the North Pacific, Science, 298(5594), 817–821, https://doi.org/10.1126/science.1074961, 2002.

Bonnet, S. and Guieu, C.: Atmospheric forcing on the annual iron cycle in the western Mediterranean Sea: A 1-year survey, J. Geophys. Res-Biogeo., 111, C09010, https://doi.org/10.1029/2005JC003213, 2006.

Bonnet, S., Guieu, C., Chiaverini, J., Ras, J. and Stock, A.: Effect of atmospheric nutrients on the autotrophic communities in a low nutrient, low chlorophyll system, Limnol. Oceanogr., 50(6), 1810–1819, https://doi.org/10.4319/lo.2005.50.6.1810, 2005.

Bosc, E., Bricaud, A. and Antoine, D.: Seasonal and interannual variability in algal biomass and primary production in the Mediterranean Sea, as derived from 4 years of SeaWiFS observations, Global Biogeochem. Cy., 18(1), GB1005, https://doi.org/10.1029/2003GB002034, 2004.

Boscolo-Galazzo, F., Crichton, K. A., Barker, S. and Pearson, P. N.: Temperature dependency of metabolic rates in the upper ocean: A positive feedback to global climate change?, Global and Planetary Change, 170, 201–212, https://doi.org/10.1016/j.gloplacha.2018.08.017,

1143   2018.

1144   Bressac, M., Guieu, C., Doxaran, D., Bourrin, F., Obolensky, G., and Grisoni, J.-M.: A

1145   mesocosm experiment coupled with optical measurements to assess the fate and sinking

1146   of atmospheric particles in clear oligotrophic waters, Geo-Mar. Lett., 32, 153–164,

1147   doi:10.1007/s00367-011- 0269-4, 2012.

1148   Bressac, M. and Guieu, C.: Post-depositional processes: What really happens to new atmospheric

1149   iron in the ocean's surface?, Global Biogeochem. Cy., 27(3), 859–870,

1150   https://doi.org/10.1002/gbc.20076, 2013.

1151   Bressac, M., Guieu, C., Doxaran, D., Bourrin, F., Desboeufs, K., Leblond, N. and Ridame, C.:

1152   Quantification of the lithogenic carbon pump following a simulated dust-deposition event

1153   in large mesocosms, Biogeosciences, 11(4), 1007–1020, https://doi.org/10.5194/bg-11-

1154   1007-2014, 2014.

1155   Bressac, M., Wagener, T., Leblond, N., Tovar-Sánchez, A., Ridame, C., Albani, S., Guasco, S.,

1156   Dufour, A., Jacquet, S., Dulac, F., Desboeufs, K., and Guieu, C.: Subsurface iron

1157   accumulation and rapid aluminium removal in the Mediterranean following African dust

1158   deposition, Biogeosciences Discussions, 1–29, https://doi.org/10.5194/bg-2021-87, 2021.

1159   Brown, J. H., Gillooly, J. F., Allen, A. P., Savage, V. M. and West, G. B.: Toward a Metabolic

1160   Theory of Ecology, Ecology, 85(7), 1771–1789, https://doi.org/10.1890/03-9000, 2004.

1161   Cael, B. B. and Follows, M. J.: On the temperature dependence of oceanic export efficiency,

1162   Geophys. Res. Lett., 43(10), 5170–5175, https://doi.org/10.1002/2016GL068877, 2016.

1163   Cael, B. B., Bisson, K. and Follows, M. J.: How have recent temperature changes affected the

1164   efficiency of ocean biological carbon export?, Limnol. Oceanogr. Lett., 2(4), 113–118,

1165   https://doi.org/10.1002/lol2.10042, 2017.

1173   Calvo-Díaz, A., Díaz-Pérez, L., Suárez, L. Á., Morán, X. A. G., Teira, E. and Marañón, E.:

1174   Decrease in the Autotrophic-to-Heterotrophic Biomass Ratio of Picoplankton in

1175   Oligotrophic Marine Waters Due to Bottle Enclosure, Appl. Environ. Microbiol., 77(16),

1176   5739–5746, https://doi.org/10.1128/AEM.00066-11, 2011.

1177   Chen, B. and Laws, E. A.: Is there a difference of temperature sensitivity between marine

1178   phytoplankton and heterotrophs?, Limnol. Oceanogr., 62(2), 806–817,

1179   https://doi.org/10.1002/lno.10462, 2017.

1180   Christaki, U., Van Wambeke, F., Lefevre, D., Lagaria, A., Prieur, L., Pujo-Pay, M.,

1181   Grattepanche, J.-D., Colombet, J., Psarra, S., Dolan, J. R., Sime-Ngando, T., Conan, P.,

1182   Weinbauer, M. G. and Moutin, T.: Microbial food webs and metabolic state across

1183   oligotrophic waters of the Mediterranean Sea during summer, Biogeosciences, 8(7),

1184   1839–1852, https://doi.org/10.5194/bg-8-1839-2011, 2011.

1185   Desboeufs, K., Leblond, N., Wagener, T., Bon Nguyen, E. and Guieu, C.: Chemical fate and

1186   settling of mineral dust in surface seawater after atmospheric deposition observed from

1187   dust seeding experiments in large mesocosms, Biogeosciences, 11(19), 5581–5594,

1188   https://doi.org/10.5194/bg-11-5581-2014, 2014.

1189   Desboeufs, K.:XXXXX, in Atmospheric Chemistry in the Mediterranean Region:

1190   Comprehensive Diagnosis and Impacts, edited by F. Dulac, S. Sauvage, and E. Hamonou,

1191   Springer, Cham, Switzerland, 2022.

1192   Dinasquet, J., Bigeard, E., Gazeau, F., Azam, F., Guieu, C., Marañón, E., Ridame, C., Van

1193   Wambeke, F., Obernosterer, I., and Baudoux, A.-C.: Impact of dust addition on the

1194   microbial food web under present and future conditions of pH and temperature,

1195   Biogeosciences Discussions, 1–48, https://doi.org/10.5194/bg-2021-143, 2021.

48

Dittmar, T., Cherrier, J. and Ludwichowski, K.-U.: The analysis of amino acids in seawater, in Practical Guidelines for the Analysis of Seawater, edited by O. Wurl, pp. 67–77, CRC Press Taylor & Francis Group, Boca Raton, FL., 2009.

Emerson, S., Quay, P., Karl, D., Winn, C., Tupas, L. and Landry, M.: Experimental determination of the organic carbon flux from open-ocean surface waters, Nature, 389(6654), 951–954, https://doi.org/10.1038/40111, 1997.

Engel, A.: Determination of marine gel particles, in Practical Guidelines for the Analysis of Seawater, edited by O. Wurl, pp. 125–142, CRC Press Taylor & Francis Group, Boca Raton, FL., 2009.

Engel, A. and Händel, N.: A novel protocol for determining the concentration and composition of sugars in particulate and in high molecular weight dissolved organic matter (HMW-DOM) in seawater, Mar. Chem., 127(1), 180–191, https://doi.org/10.1016/j.marchem.2011.09.004, 2011.

Feliú, G., Pagano, M., Hidalgo, P. and Carlotti, F.: Structure and function of epipelagic mesozooplankton and their response to dust deposition events during the spring PEACETIME cruise in the Mediterranean Sea, Biogeosciences, 17, 5417–5441, https://doi.org/10.5194/bg-17-5417-2020, 2020.

Ferguson, R. L., Buckley, E. N. and Palumbo, A. V.: Response of marine bacterioplankton to differential filtration and confinement., Appl. Environ. Microbiol., 47(1), 49–55, 1984.

Friedlingstein, P., O'Sullivan, M., Jones, M. W., Andrew, R. M., Hauck, J., Olsen, A., Peters, G. P., Peters, W., Pongratz, J., Sitch, S., Le Quéré, C., Canadell, J. G., Ciais, P., Jackson, R. B., Alin, S., Aragão, L. E. O. C., Arneth, A., Arora, V., Bates, N. R., Becker, M., Benoit-Cattin, A., Bittig, H. C., Bopp, L., Bultan, S., Chandra, N., Chevallier, F., Chini, L. P.,

Evans, W., Florentie, L., Forster, P. M., Gasser, T., Gehlen, M., Gilfillan, D., Gkritzalis,

T., Gregor, L., Gruber, N., Harris, I., Hartung, K., Haverd, V., Houghton, R. A., Ilyina,

T., Jain, A. K., Joetzjer, E., Kadono, K., Kato, E., Kitidis, V., Korsbakken, J. I.,

Landschützer, P., Lefèvre, N., Lenton, A., Lienert, S., Liu, Z., Lombardozzi, D., Marland,

G., Metzl, N., Munro, D. R., Nabel, J. E. M. S., Nakaoka, S.-I., Niwa, Y., O'Brien, K.,

Ono, T., Palmer, P. I., Pierrot, D., Poulter, B., Resplandy, L., Robertson, E., Rödenbeck,

C., Schwinger, J., Séférian, R., Skjelvan, I., Smith, A. J. P., Sutton, A. J., Tanhua, T.,

Tans, P. P., Tian, H., Tilbrook, B., van der Werf, G., Vuichard, N., Walker, A. P.,

Wanninkhof, R., Watson, A. J., Willis, D., Wiltshire, A. J., Yuan, W., Yue, X. and

Zaehle, S.: Global Carbon Budget 2020, Earth Syst. Sci. Data, 12(4), 3269–3340,

https://doi.org/10.5194/essd-12-3269-2020, 2020.

Garcia-Corral, L. S., Holding, J. M., Carrillo-de-Albornoz, P., Steckbauer, A., Pérez-Lorenzo,

M., Navarro, N., Serret, P., Gasol, J. M., Morán, X. A. G., Estrada, M., Fraile-Nuez, E.,

Benítez-Barrios, V., Agusti, S. and Duarte, C. M.: Temperature dependence of plankton

community metabolism in the subtropical and tropical oceans, Global Biogeochem. Cy.,

31(7), 1141–1154, https://doi.org/10.1002/2017GB005629, 2017.

Gazeau, F., Ridame, C., Van Wambeke, F., Alliouane, S., Stolpe, C., Irisson, J.-O., Marro, S.,

Grisoni, J.-M., De Liège, G., Nunige, S., Djaoudi, K., Pulido-Villena, E., Dinasquet, J.,

Obernosterer, I., Catala, P. and Guieu, C.: Impact of dust addition on Mediterranean

plankton communities under present and future conditions of pH and temperature: an

overview, Biogeosciences, 18, 1–24, https://doi.org/10.5194/bg-18-1-2021, 2021.

Gillikin, D. P. and Bouillon, S.: Determination of $\delta^{18}O$ of water and $\delta^{13}C$ of dissolved inorganic

carbon using a simple modification of an elemental analyser-isotope ratio mass

1267   spectrometer: an evaluation, Rapid Commiun. Mass Sp., 21(8), 1475–1478,

1268   https://doi.org/10.1002/rcm.2968, 2007.

1269 Gillooly, J. F., Brown, J. H., West, G. B., Savage, V. M. and Charnov, E. L.: Effects of size and

1270   temperature on metabolic rate, Science, 293(5538), 2248–2251,

1271   https://doi.org/10.1126/science.1061967, 2001.

1272 del Giorgio, P. and Williams, P.: Respiration in Aquatic Ecosystems, Oxford University Press.

1273   https://oxford.universitypressscholarship.com/view/10.1093/acprof:oso/9780198527084.

1274   001.0001/acprof-9780198527084, last access: 22 January 2021, 2005.

1275 Guieu, C. and Ridame, C.: Impact of atmospheric deposition on marine chemistry and

1276   biogeochemistry, in Atmospheric Chemistry in the Mediterranean Region:

1277   Comprehensive Diagnosis and Impacts, edited by F. Dulac, S. Sauvage, and E. Hamonou,

1278   Springer, Cham, Switzerland, 2020.

1279 Guieu, C., Loye-Pilot, M. D., Benyahya, L. and Dufour, A.: Spatial variability of atmospheric

1280   fluxes of metals (Al, Fe, Cd, Zn and Pb) and phosphorus over the whole Mediterranean

1281   from a one-year monitoring experiment: Biogeochemical implications, Mar. Chem.,

1282   120(1–4), 164–178, https://doi.org/10.1016/j.marchem.2009.02.004, 2010.

1283 Guieu, C., Ridame, C., Pulido-Villena, E., Bressac, M., Desboeufs, K. and Dulac, F.: Impact of

1284   dust deposition on carbon budget: a tentative assessment from a mesocosm approach,

1285   Biogeosciences, 11(19), 5621–5635, 2014a.

1286 Guieu, C., Aumont, O., Paytan, A., Bopp, L., Law, C. S., Mahowald, N., Achterberg, E. P.,

1287   Marañón, E., Salihoglu, B., Crise, A., Wagener, T., Herut, B., Desboeufs, K., Kanakidou,

1288   M., Olgun, N., Peters, F., Pulido-Villena, E., Tovar-Sanchez, A. and Völker, C.: The

1289   significance of the episodic nature of atmospheric deposition to Low Nutrient Low

Chlorophyll regions, Global Biogeochemical Cycles, 28(11), 1179–1198,

https://doi.org/10.1002/2014GB004852, 2014b.

Guieu, C., D'Ortenzio, F., Dulac, F., Taillandier, V., Doglioli, A., Petrenko, A., Barrillon, S.,

Mallet, M., Nabat, P. and Desboeufs, K.: Process studies at the air-sea interface after

atmospheric deposition in the Mediterranean Sea: objectives and strategy of the

PEACETIME oceanographic campaign (May–June 2017), Biogeosciences, 2020(17),

5563–5585, https://doi.org/10.5194/bg-17-5563-2020, 2020a.

Guieu, C., Desboeufs, K., Albani, S., Alliouane, S., Aumont, O., Barbieux, M., Barrillon, S.,

Baudoux, A.-C., Berline, L., Bhairy, N., Bigeard. E., Bloss, M., Bressac, M., Brito, J.,

Carlotti, F., de Liege, G., Dinasquet, J., Djaoudi, K., Doglioli, A., D'Ortenzio, F.,

Doussin, J.-F., Duforet, L., Dulac, F., Dutay, J.-C., Engel, A., Feliu-Brito, G., Ferre, H.,

Formenti, P., Fu, F., Garcia, D., Garel, D., Gazeau, F., Giorio, C., Gregori, G., Grisoni,

J.-M., Guasco, S., Guittonneau, J., Haëntjens, N., Heimburger, L.-E., Helias, S., Jacquet,

S., Laurent, B., Leblond, N., Lefevre, D., Mallet , M., Marañón, E., Nabat, P., Nicosia,

A., Obernosterer, I., Perez, L., M., Petrenko, A., Pulido-Villena, E., Raimbault, P.,

Ridame, C., Riffault, V., Rougier, G., Rousselet, L., Roy-Barman, M., Saiz- Lopez, A.,

Schmechtig, C., Sellegri, K., Siour, G., Taillandier, V., Tamburini , C., Thyssen, M.,

Tovar-Sanchez, A., Triquet, S., Uitz, J., Van Wambeke, F., Wagener, T., and Zaencker,

B.: Bio- geochemical dataset collected during the PEACETIME cruise, SEANOE

[Dataset], https://doi.org/10.17882/75747, 2020b.

Hein, M. and Sand-Jensen, K.: CO_2 increases oceanic primary production, Nature, 388(6642),

526–527, 1997.

Herut, B., Zohary, T., Krom, M. D., Mantoura, R. F. C., Pitta, P., Psarra, S., Rassoulzadegan, F.,
Tanaka, T. and Frede Thingstad, T.: Response of East Mediterranean surface water to
Saharan dust: On-board microcosm experiment and field observations, Deep Sea
Research Part II: Topical Studies in Oceanography, 52(22), 3024–3040,
https://doi.org/10.1016/j.dsr2.2005.09.003, 2005.

Herut, B., Rahav, E., Tsagaraki, T. M., Giannakourou, A., Tsiola, A., Psarra, S., Lagaria, A.,
Papageorgiou, N., Mihalopoulos, N., Theodosi, C. N., Violaki, K., Stathopoulou, E.,
Scoullos, M., Krom, M. D., Stockdale, A., Shi, Z., Berman-Frank, I., Meador, T. B.,
Tanaka, T. and Paraskevi, P.: The potential impact of Saharan dust and polluted aerosols
on microbial populations in the East Mediterranean Sea, an overview of a mesocosm
experimental approach, Front. Mar. Sci., 3, 226,
https://doi.org/10.3389/fmars.2016.00226, 2016.

Hoppe, H.-G.: Significance of exoenzymatic activities in the ecology of brackish water:
measurements by means of methylumbelliferyl-substrates, Mar. Ecol. Prog. Ser., 11(3),
299–308, 1983.

IPCC: Climate Change 2013: The Physical Science Basis. Contri- bution of Working Group I to
the Fifth Assessment Report of the Intergovernmental Panel on Climate Change, edited
by: Stocker, T. F., Qin, D., Plattner, G.-K., Tignor, M., Allen, S. K., Boschung, J.,
Nauels, A., Xia, Y., Bex, V., and Midgley, P. M., Cambridge University Press,
Cambridge, United Kingdom and New York, NY, USA, 1535 pp., 2013.

Irwin, A. J. and Oliver, M. J.: Are ocean deserts getting larger?, Geophys. Res. Lett., 36,
L18609, https://doi.org/10.1029/2009gl039883, 2009.

Jickells, T. and Moore, C. M.: The importance of atmospheric deposition for ocean productivity,

Annu. Rev. Ecol. Evol. S., 46(1), 481–501, https://doi.org/10.1146/annurev-ecolsys-112414-054118, 2015.

Kirchman, D. L., Kemp, P., Sherr, B., Sherr, E. and Cole, J.: Leucine incorporation as a measure of biomass production by heterotrophic bacteria, in Handbook of methods in aquatic microbial ecology, pp. 509–512, CRC Press, https://doi.org/10.1201/9780203752746-59, 1993.

Knap, A., Michaels, A., Close, A., Ducklow, H. and Dickson, A.: Protocols for the Joint Global Ocean Flux Study (JGOFS) Core Measurements, UNESCO 1994., 1996.

Kouvarakis, G., Mihalopoulos, N., Tselepides, A. and Stavrakakis, S.: On the importance of atmospheric inputs of inorganic nitrogen species on the productivity of the Eastern Mediterranean Sea, Global Biogeochem. Cy., 15(4), 805–817, https://doi.org/10.1029/2001GB001399, 2001.

Kroeker, K. J., Kordas, R. L., Crim, R., Hendriks, I. E., Ramajo, L., Singh, G. S., Duarte, C. M. and Gattuso, J. P.: Impacts of ocean acidification on marine organisms: quantifying sensitivities and interaction with warming, Glob. Change Biol., 19(6), 1884–1896, https://doi.org/10.1111/gcb.12179, 2013.

Langer, G., Nehrke, G., Probert, I., Ly, J. and Ziveri, P.: Strain-specific responses of *Emiliania huxleyi* to changing seawater carbonate chemistry, Biogeosciences, 6(11), 2637–2646, https://doi.org/10.5194/bg-6-2637-2009, 2009.

Laurent, B., Audoux, T., Bibi, M., Dulac, F. and Bergametti, G.: Mass deposition in the Mediterranean region, in Atmospheric Chemistry in the Mediterranean Region: Comprehensive Diagnosis and Impacts, edited by F. Dulac, S. Sauvage, and E. Hamonou, Springer, Cham, Switzerland, 2021.

54

Lazzari, P., Solidoro, C., Salon, S. and Bolzon, G.: Spatial variability of phosphate and nitrate in the Mediterranean Sea: A modeling approach, Deep-Sea Res. Pt I, 108, 39–52, https://doi.org/10.1016/j.dsr.2015.12.006, 2016.

Lekunberri, I., Lefort, T., Romero, E., Vázquez-Domínguez, E., Romera-Castillo, C., Marrasé, C., Peters, F., Weinbauer, M. and Gasol, J. M.: Effects of a dust deposition event on coastal marine microbial abundance and activity, bacterial community structure and ecosystem function, J. Plankton Res., 32(4), 381–396, https://doi.org/10.1093/plankt/fbp137, 2010.

Lemée, R., Rochelle-Newall, E., Van Wambeke, F., Pizay, M., Rinaldi, P. and Gattuso, J.-P.: Seasonal variation of bacterial production, respiration and growth efficiency in the open NW Mediterranean Sea, Aquat. Microb. Ecol., 29, 227–237, https://doi.org/10.3354/ame029227, 2002.

Lewandowska, A. M., Boyce, D. G., Hofmann, M., Matthiessen, B., Sommer, U. and Worm, B.: Effects of sea surface warming on marine plankton, Ecol. Lett., 17(5), 614–623, https://doi.org/10.1111/ele.12265, 2014.

Lindroth, P. and Mopper, K.: High performance liquid chromatographic determination of subpicomole amounts of amino acids by precolumn fluorescence derivatization with o-phthaldialdehyde, Anal. Chem., 51(11), 1667–1674, https://doi.org/10.1021/ac50047a019, 1979.

Longhurst, A., Sathyendranath, S., Platt, T. and Caverhill, C.: An estimate of global primary production in the ocean from satellite radiometer data, J. Plankton Res., 17(6), 1245–1271, https://doi.org/10.1093/plankt/17.6.1245, 1995.

Lopez-Urrutia, A. and Moran, X. A. G.: Resource limitation of bacterial production distorts the

temperature dependence of oceanic carbon cycling, Ecology, 88(4), 817–822, 2007.

Louis, J., Pedrotti, M. L., Gazeau, F. and Guieu, C.: Experimental evidence of formation of transparent exopolymer particles (TEP) and POC export provoked by dust addition under current and high pCO$_2$ conditions, PLOS ONE, 12(2), e0171980, https://doi.org/10.1371/journal.pone.0171980, 2017.

Loÿe-Pilot, M. D. and Martin, J. M.: Saharan Dust Input to the Western Mediterranean: An Eleven Years Record in Corsica, in The Impact of Desert Dust Across the Mediterranean, edited by S. Guerzoni and R. Chester, pp. 191–199, Springer Netherlands, Dordrecht, https://doi.org/10.1007/978-94-017-3354-0_18, 1996.

Mackey, K., Morris, J. J., Morel, F. and Kranz, S.: Response of photosynthesis to ocean acidification, Oceanography, 25(2), 74–91, https://doi.org/10.5670/oceanog.2015.33, 2015.

Marañón, E., Fernández, A., Mouriño-Carballido, B., MartÍnez-GarcÍa, S., Teira, E., Cermeño, P., Chouciño, P., Huete-Ortega, M., Fernández, E., Calvo-DÍaz, A., Morán, X. A. G., Bode, A., Moreno-Ostos, E., Varela, M. M., Patey, M. D. and Achterberg, E. P.: Degree of oligotrophy controls the response of microbial plankton to Saharan dust, Limnol. Oceanogr., 55(6), 2339–2352, https://doi.org/10.4319/lo.2010.55.6.2339, 2010.

Marañón, E., Lorenzo, M. P., Cermeño, P. and Mouriño-Carballido, B.: Nutrient limitation suppresses the temperature dependence of phytoplankton metabolic rates, The ISME Journal, 12(7), 1836–1845, https://doi.org/10.1038/s41396-018-0105-1, 2018.

Marañón, E., Van Wambeke, F., Uitz, J., Boss, E. S., Dimier, C., Dinasquet, J., Engel, A., Haëntjens, N., Pérez-Lorenzo, M., Taillandier, V., and Zäncker, B.: Deep maxima of phytoplankton biomass, primary production and bacterial production in the

56

Mediterranean Sea, Biogeosciences, 18, 1749–1767, https://doi.org/10.5194/bg-18-1749-2021, 2021.

Mari, X.: Carbon content and C:N ratio of transparent exopolymeric particles (TEP) produced by bubbling exudates of diatoms, Mar. Ecol. Prog. Ser., 183, 59–71, https://doi.org/10.3354/meps183059, 1999.

Markaki, Z., Oikonomou, K., Kocak, M., Kouvarakis, G., Chaniotaki, A., Kubilay, N. and Mihalopoulos, N.: Atmospheric deposition of inorganic phosphorus in the Levantine Basin, eastern Mediterranean: Spatial and temporal variability and its role in seawater productivity, Limnol. Oceanogr., 48(4), 1557–1568, https://doi.org/10.4319/lo.2003.48.4.1557, 2003.

Maugendre, L., Gattuso, J.-P., Louis, J., de Kluijver, A., Marro, S., Soetaert, K. and Gazeau, F.: Effect of ocean warming and acidification on a plankton community in the NW Mediterranean Sea, ICES J. Mar. Sci., 72(6), 1744–1755, https://doi.org/10.1093/icesjms/fsu161, 2015.

Maugendre, L., Gattuso, J.-P., Poulton, A. J., Dellisanti, W., Gaubert, M., Guieu, C. and Gazeau, F.: No detectable effect of ocean acidification on plankton metabolism in the NW oligotrophic Mediterranean Sea: Results from two mesocosm studies, Estuar. Coast. Shelf S., 186, 89–99, https://doi.org/10.1016/j.ecss.2015.03.009, 2017a.

Maugendre, L., Guieu, C., Gattuso, J.-P. and Gazeau, F.: Ocean acidification in the Mediterranean Sea: Pelagic mesocosm experiments. A synthesis, Estuar. Coast. Shelf S., 186, 1–10, https://doi.org/10.1016/j.ecss.2017.01.006, 2017b.

McClain, C. R., Signorini, S. R., and Christian, J. R.: Subtropical gyre variability observed by ocean-color satellites, Deep-Sea Res. Pt II, 51, 281–301, https://doi.org/10.1016/j.dsr2.2003.08.002, 2004.

Mercado, J. M., Sobrino, C., Neale, P. J., Segovia, M., Reul, A., Amorim, A. L., Carrillo, P., Claquin, P., Cabrerizo, M. J., León, P., Lorenzo, M. R., Medina-Sánchez, J. M., Montecino, V., Napoleon, C., Prasil, O., Putzeys, S., Salles, S. and Yebra, L.: Effect of CO_2, nutrients and light on coastal plankton. II. Metabolic rates, Aquat. Biol., 22, 43–57, https://doi.org/10.3354/ab00606, 2014.

Mills, M. M., Moore, C. M., Langlois, R., Milne, A., Achterberg, E., Nachtigall, K., Lochte, K., Geider, R. J. and La, R. J.: Nitrogen and phosphorus co-limitation of bacterial productivity and growth in the oligotrophic subtropical North Atlantic, Limnol. Oceanogr., 53(2), 824–834, https://doi.org/10.4319/lo.2008.53.2.0824, 2008.

Mosseri, J., Quéguiner, B., Rimmelin, P., Leblond, N. and Guieu, C.: Silica fluxes in the northeast Atlantic frontal zone of Mode Water formation (38°–45°N, 16°–22°W) in 2001–2002, J. Geophys. Res-Oceans, 110, C07S19, https://doi.org/10.1029/2004JC002615, 2005.

Moulin, C. and Chiapello, I.: Impact of human-induced desertification on the intensification of Sahel dust emission and export over the last decades, Geophys. Res. Lett., 33(18), L18808, https://doi.org/10.1029/2006GL025923, 2006.

Moutin, T. and Raimbault, P.: Primary production, carbon export and nutrients availability in western and eastern Mediterranean Sea in early summer 1996 (MINOS cruise), J. Mar. Syst., 33–34, 273–288, https://doi.org/10.1016/S0924-7963(02)00062-3, 2002.

Moutin, T., Thingstad, T. F., Wambeke, F. V., Marie, D., Slawyk, G., Raimbault, P. and

Claustre, H.: Does competition for nanomolar phosphate supply explain the predominance of the cyanobacterium Synechococcus?, Limnol. Oceanogr., 47(5), 1562–1567, https://doi.org/10.4319/lo.2002.47.5.1562, 2002.

Müren, U., Berglund, J., Samuelsson, K. and Andersson, A.: Potential Effects of Elevated Sea-Water Temperature on Pelagic Food Webs, Hydrobiologia, 545(1), 153–166, https://doi.org/10.1007/s10750-005-2742-4, 2005.

Passow, U. and Carlson, C. A.: The biological pump in a high CO_2 world, Mar. Ecol. Prog. Ser., 470, 249–271, 2012.

Polovina, J. J., Howell, E. A. and Abecassis, M.: Ocean's least productive waters are expanding, Geophys. Res. Lett., 35(3), L03618, https://doi.org/10.1029/2007gl031745, 2008.

Pulido-Villena, E., Wagener, T. and Guieu, C.: Bacterial response to dust pulses in the western Mediterranean: Implications for carbon cycling in the oligotrophic ocean, Global Biogeochem. Cy., 22, GB1020, https://doi.org/10.1029/2007gb003091, 2008

Pulido-Villena, E., Baudoux, A.-C., Obernosterer, I., Landa, M., Caparros, J., Catala, P., Georges, C., Harmand, J. and Guieu, C.: Microbial food web dynamics in response to a Saharan dust event: results from a mesocosm study in the oligotrophic Mediterranean Sea, Biogeosciences, 11(19), 5607–5619, 2014.

Regaudie-de-Gioux, A. and Duarte, C. M.: Temperature dependence of planktonic metabolism in the ocean, Global Biogeochem. Cy., 26(1), GB1015, https://doi.org/10.1029/2010GB003907, 2012.

Regaudie-de-Gioux, A., Vaquer-Sunyer, R. and Duarte, C. M.: Patterns in planktonic metabolism in the Mediterranean Sea, Biogeosciences, 6(12), 3081–3089, https://doi.org/10.5194/bg-6-3081-2009, 2009.

Ridame, C. and Guieu, C.: Saharan input of phosphate to the oligotrophic water of the open

western Mediterranean Sea, Limnol. Oceanogr., 47(3), 856–869, 2002.

Riebesell, U., Schulz, K. G., Bellerby, R. G. J., Botros, M., Fritsche, P., Meyerhofer, M., Neill,

C., Nondal, G., Oschlies, A., Wohlers, J. and Zollner, E.: Enhanced biological carbon

consumption in a high CO_2 ocean, Nature, 450(7169), 545-U10, 2007.

Roshan, S. and DeVries, T.: Efficient dissolved organic carbon production and export in the

oligotrophic ocean, Nat. Commun., 8, 2036, https://doi.org/10.1038/s41467-017-02227-3,

2017.

Smith, D. C. and Azam, F.: A simple, economical method for measuring bacterial protein

synthesis rates in seawater using ^{3}H-leucine, Marine Microbial Food Webs, 6(2), 107–

114, 1992.

Schneider, C. A., Rasband, W. S., and Eliceiri, K. W.: NIH Image to ImageJ: 25 years of Image

Analysis, Nat. Methods, 9, 671–675, 2012.

Tanaka, T., Thingstad, T. F., Christaki, U., Colombet, J., Cornet-Barthaux, V., Courties, C.,

Grattepanche, J.-D., Lagaria, A., Nedoma, J., Oriol, L., Psarra, S., Pujo-Pay, M. and

Wambeke, F. V.: Lack of P-limitation of phytoplankton and heterotrophic prokaryotes in

surface waters of three anticyclonic eddies in the stratified Mediterranean Sea,

Biogeosciences, 8(2), 525–538, https://doi.org/10.5194/bg-8-525-2011, 2011.

Ternon, E., Guieu, C., Loÿe-Pilot, M.-D., Leblond, N., Bosc, E., Gasser, B., Miquel, J.-C. and

Martín, J.: The impact of Saharan dust on the particulate export in the water column of

the North Western Mediterranean Sea, Biogeosciences, 7(3), 809–826,

https://doi.org/10.5194/bg-7-809-2010, 2010.

Thingstad, T. F., Krom, M. D., Mantoura, R. F. C., Flaten, G. a. F., Groom, S., Herut, B., Kress,

N., Law, C. S., Pasternak, A., Pitta, P., Psarra, S., Rassoulzadegan, F., Tanaka, T.,

Tselepides, A., Wassmann, P., Woodward, E. M. S., Riser, C. W., Zodiatis, G. and

Zohary, T.: Nature of Phosphorus Limitation in the Ultraoligotrophic Eastern

Mediterranean, Science, 309(5737), 1068–1071, https://doi.org/10.1126/science.1112632,

2005.

Van Wambeke, F., Taillandier, V., Deboeufs, K., Pulido-Villena, E., Dinasquet, J., Engel, A.,

Marañón, E., Ridame, C., and Guieu, C.: Influence of atmospheric deposition on

biogeochemical cycles in an oligotrophic ocean system, Biogeosciences Discuss.

[preprint], https://doi.org/10.5194/bg-2020-411, in review, 2020.

Van Wambeke, F., Pulido, E., Catala, P., Dinasquet, J., Djaoudi, K., Engel, A., Garel, M.,

Guasco, S., Marie, B., Nunige, S., Taillandier, V., Zäncker, B., and Tamburini, C.:

Spatial patterns of ectoenzymatic kinetics in relation to biogeochemical properties in the

Mediterranean Sea and the concentration of the fluorogenic substrate used,

Biogeosciences, 18, 2301–2323, https://doi.org/10.5194/bg-18-2301-2021, 2021.

Wang, Q., Lyu, Z., Omar, S., Cornell, S., Yang, Z. and Montagnes, D. J. S.: Predicting

temperature impacts on aquatic productivity: Questioning the metabolic theory of

ecology's "canonical" activation energies, Limnol. Oceanogr., 64(3), 1172–1185,

https://doi.org/10.1002/lno.11105, 2019.

Zobell, C. E. and Anderson, D. Q.: Observations on the multiplication of bacteria in different

volumes of stored sea water and the influence of oxygen tension and solid surfaces, The

Biological Bulletin, 71(2), 324–342, https://doi.org/10.2307/1537438, 1936.

Tables

Table 1. Initial chemical and biological stocks as measured while filling the tanks (initial conditions in pumped surface water; sampling time: t-12h). NO_x: nitrate + nitrite, DIP: dissolved inorganic phosphorus, $Si(OH)_4$: silicate, POC: particulate organic carbon, DOC: dissolved organic carbon, TEP: transparent exopolymer particles, TChl$a$: total chlorophyll a. Values shown for ^{14}C incorporation rates, percentages of extracellular release (%PER) as well as for net community production (NCP), community respiration (CR) and gross primary production (GPP) were estimated from samples taken at t0 in the control tanks. For heterotrophic bacterial production (BP), rates were estimated from seawater sampled at t-12h.

	Sampling station	TYR	ION	FAST
	Coordinates (decimal)	39.34 N, 12.60 E	35.49 N, 19.78 E	37.95 N, 2.90 N
	Bottom depth (m)	3395	3054	2775
	Day and time of pumping (local time)	17/05/2017 17:00	25/05/2017 17:00	02/06/2017 21:00
	Temperature (°C)	20.6	21.2	21.5
	Salinity	37.96	39.02	37.07
Stocks	NO_x (nmol L^{-1})	14.0	18.0	59.0
	DIP (nmol L^{-1})	17.1	6.5	12.9
	$Si(OH)_4$ (µmol L^{-1})	1.0	0.96	0.64

	POC (μmol L^{-1})	12.9	8.5	6.0
	DOC (μmol L^{-1})	72.2	70.2	69.6
	TEP (x 10^6 L^{-1})	6.8	3.8	3.7
	TChl$a$ (μg L^{-1})	0.063	0.066	0.072
	Heterotrophic prokaryotes abundance (x 10^5 cell mL^{-1})	4.79	2.14	6.15
Processes	^{14}C-based total particulate production (μg C L^{-1} h^{-1})	0.08 ± 0.03	0.14 ± 0.04	0.15 ± 0.04
	^{14}C-based > 2 μm particulate production (μg C L^{-1} h^{-1})	0.07 ± 0.02	0.11 ± 0.02	0.11 ± 0.02
	^{14}C-based < 2 μm particulate production (μg C L^{-1} h^{-1})	0.01 ± 0.01	0.04 ± 0.02	0.05 ± 0.01
	%PER	60 ± 20	45 ± 3	32 ± 23
	NCP (μmol O$_2$ L^{-1} d^{-1})	-1.9 ± 0.3	-0.2 ± 0.2	-0.8 ± 0.9
	CR (μmol O$_2$ L^{-1} d^{-1})	-2.6 ± 0.1	-1.2 ± 0.5	-1.9 ± 1.6
	GPP (μmol O$_2$ L^{-1} d^{-1})	0.7 ± 0.4	1.1 ± 0.3	1.1 ± 0.7
	BP (ng C L^{-1} h^{-1})	11.6	15.2	34.6

1625

1626 Table 2. Heterotrophic bacterial production (BP) growth rates (μ_{BP} in h^{-1}) estimated from the

1627 exponential phase of BP growth, observable from at least four sampling points, between t0 and

1628 t12h, during the three experiments (TYR, ION and FAST) in the six tanks (controls: C1, C2; dust

1629 addition under present conditions of temperature and pH: D1, D2; dust addition under future

1630 conditions of temperature and pH: G1 and G2). Values ± SE are shown.

		μ_{BP}	
	TYR	ION	FAST
C1	0.076 ± 0.025	0.042 ± 0.007	0.020 ± 0.003
C2	0.066 ± 0.018	0.041 ± 0.005	0.026 ± 0.004
D1	0.117 ± 0.008	0.095 ± 0.020	0.089 ± 0.014
D2	0.194 ± 0.020	0.145 ± 0.007	0.090 ± 0.007
G1	0.164 ± 0.020	0.126 ± 0.011	0.124 ± 0.005
G2	0.150 ± 0.003	0.137 ± 0.033	0.163 ± 0.014

1631

Table 3. Estimated bacterial growth efficiency (BGE in %) during the course of the three experiments (TYR, ION and FAST) in the six tanks (controls: C1, C2; dust addition under present conditions of temperature and pH: D1, D2; dust addition under future conditions of temperature and pH: G1 and G2). BGE was calculated based on integrated heterotrophic bacterial production (BP) and community respiration (CR) rates by applying a bacterial respiration to CR ratio of 0.7 and a respiratory quotient of 0.8 (see Material and Methods).

Bacterial growth efficiency (BGE)		
	TYR	ION	FAST
C1	11.1	9.8	15.4
C2	11.7	14.5	22.0
D1	31.8	21.0	17.3
D2	32.3	30.6	19.9
G1	39.3	35.2	37.6
G2	32.5	34.8	38.1

Figure caption

Fig. 1. Location of the sampling stations in the Mediterranean Sea on board the R/V *Pourquoi Pas?* during the PEACETIME cruise. Background shows satellite-derived surface chlorophyll *a* concentration averaged over the entire duration of the cruise (courtesy of Louise Rousselet).

Fig. 2. Dissolved organic carbon (DOC) concentrations and ratio between total hydrolysable amino acids (TAA) and DOC concentrations measured in the six tanks (controls: C1, C2; dust addition under present conditions of temperature and pH: D1, D2; dust addition under future conditions of temperature and pH: G1 and G2) during the three experiments (TYR, ION and FAST). The dashed vertical line indicates the time of seeding (after t0).

Fig. 3. Particulate organic carbon (POC) concentrations and transparent exopolymer particle carbon content (TEP-C) measured in the six tanks (controls: C1, C2; dust addition under present conditions of temperature and pH: D1, D2; dust addition under future conditions of temperature and pH: G1 and G2) during the three experiments (TYR, ION and FAST). The dashed vertical line indicates the time of seeding (after t0).

Fig. 4. ^{14}C-based production rates (A: < 2 µm and B: > 2 µm size fractions, C: total particulate) estimated from 8 h incubations on samples taken in the six tanks (controls: C1, C2; dust addition under present conditions of temperature and pH: D1, D2; dust addition under future conditions of temperature and pH: G1 and G2) during the three experiments (TYR, ION and FAST). The percentage of extracellular release (D, %PER) is also shown.

Fig. 5. Incorporation of ^{13}C into particulate organic carbon (δ^{13}C-POC) in the six tanks (controls: C1, C2; dust addition under present conditions of temperature and pH: D1, D2; dust addition

1664 under future conditions of temperature and pH: G1 and G2) during the three experiments (TYR,

1665 ION and FAST). The dashed vertical line indicates the time of seeding (after t0).

1666 Fig. 6. A: Net community production (NCP), B: community respiration (CR) and C: gross

1667 primary production (GPP) rates estimated using the oxygen light-dark method (24 h incubations)

1668 on samples taken in the six tanks (C1, C2, D1, D2, G1 and G2) during the three experiments

1669 (TYR, ION and FAST).

1670 Fig. 7. Heterotrophic bacterial production rates (BP) and cell-specific maximum hydrolysis

1671 velocity (Vm) of the alkaline phosphatase (both over 1-2 h incubations) on samples taken in the

1672 six tanks (C1, C2, D1, D2, G1 and G2) during the three experiments (TYR, ION and FAST).

1673 Fig. 8. Total mass and organic matter fluxes measured in the sediment traps at the end of the

1674 three experiments (TYR, ION and FAST) in the six tanks (C1, C2, D1, D2, G1 and G2).

1675 Fig. 9. Relative difference (%) between integrated rates measured in tanks D (D1, D2; dust

1676 addition under present conditions of temperature and pH) and G (G1, G2; dust addition under

1677 future conditions of temperature and pH) as compared to the controls (C1, C2) during the three

1678 experiments (TYR, ION and FAST). Vertical boxes represent the range observed between the
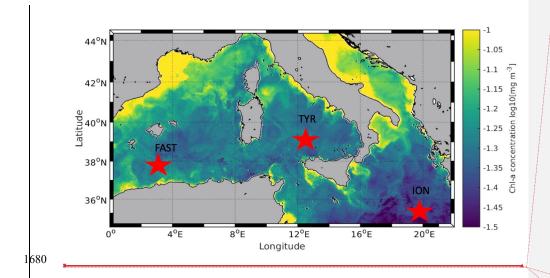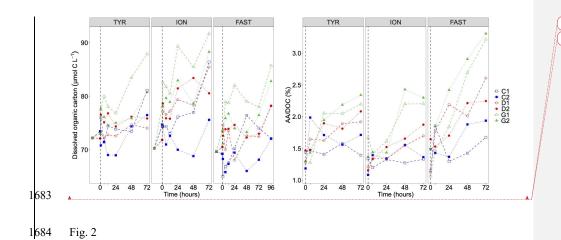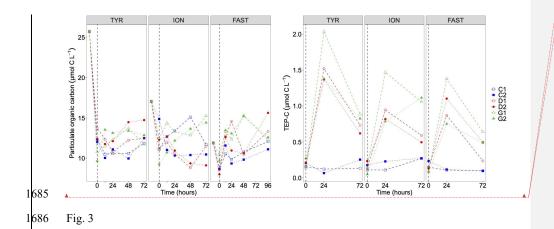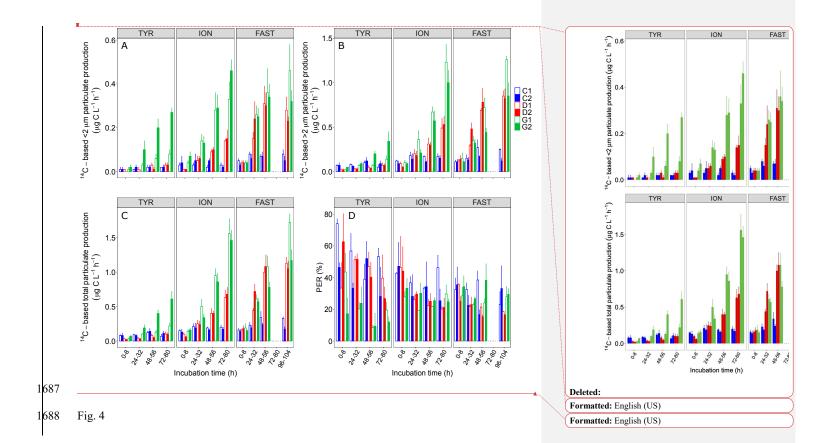
1679 two replicates per treatment.

1680

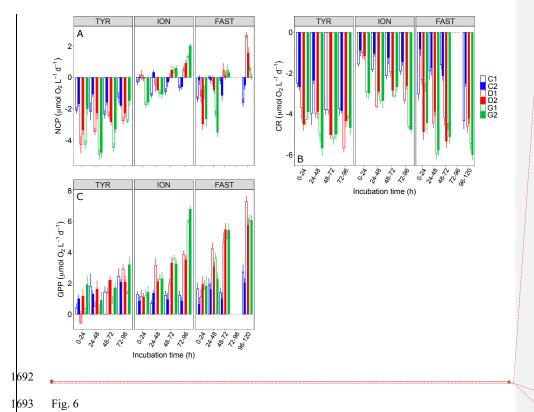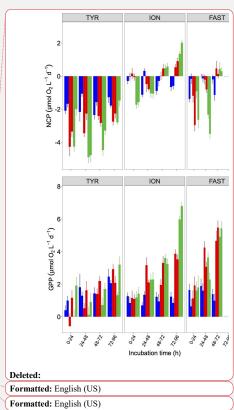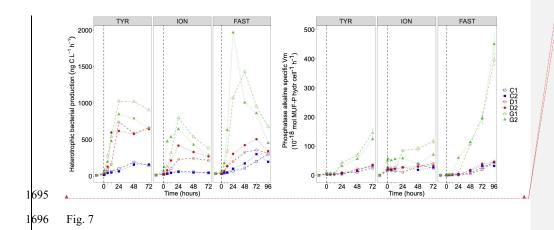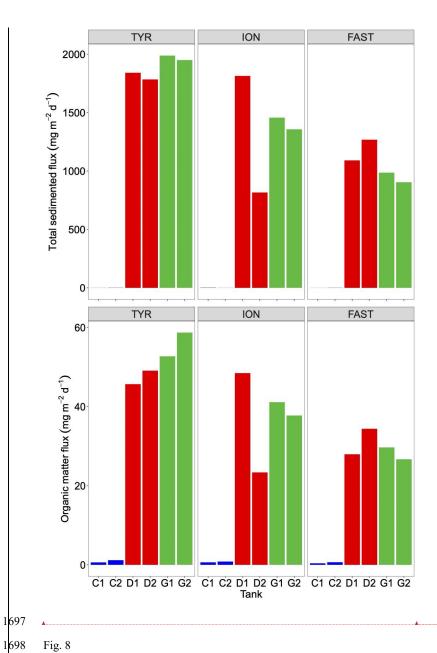1681   Fig. 1

68

1683

1684   Fig. 2

1685

1686   Fig. 3

1687

1688   Fig. 4

Deleted:

Formatted: English (US)

Formatted: English (US)

1690

1691   Fig. 5

72

1692

1693   Fig. 6

1696   Fig. 7

1697

1698   Fig. 8

75

1699

1700   Fig. 9

76